Assessment of Metabolism and Circadian Rhythm in Frontotemporal Dementia Using a Drosophila melanogaster Animal Model

Assessment of Metabolism and Circadian Rhythm in Frontotemporal Dementia Using a *Drosophila melanogaster* Animal Model

Samantha Nicodemus

A Thesis in the Field of Biology

for the Degree of Master of Liberal Arts in Extension Studies

Harvard University

May 2024

Abstract

The purpose of this behavioral study was to establish proofs of concept in metabolism and circadian rhythm in Frontotemporal Dementia (FTD) using a *Drosophila melanogaster* animal model that had been genetically modified using the UAS-*GAL4* system to have an overexpression of the Chromosome 9 Open Reading Frame 72 protein (*C9ORF72*). FTD is a progressive neurodegenerative disease, resulting in degeneration of the frontal cortex and the temporal lobe regions of the brain. Currently, there is no cure or treatment for FTD patients (Yang et al., 2020). The hexanucleotide repeat expansion in *C9ORF2* is the most common genetic cause of sporadic and familial FTD cases (Sha et al., 2012). It is hypothesized the expansion in *C9ORF72* leads to synthesis of toxic dipeptide repeats which contribute further to FTD pathology (Freibaum & Taylor, 2017). Recent research has shown inhibition of serine and arginine rich splicing protein 1 (*SRSF1*) or impeding the interaction of *SRSF1* with nuclear RNA Export Factor 1 abrogates translocation of *C9ORF72* to the cytoplasm, leads to the synthesis of dipeptide repeats, and mitigates neurotoxicity in *Drosophila melanogaster* (Hautbergue et al., 2017). There are unanswered questions regarding the effect *C9ORF72* has on behavior with respect to metabolism and circadian rhythm. Results from this study showed an alteration in circadian rhythm in pathological mutant *Drosophila* compared to non-pathological *Drosophila melanogaster* aged one day and maintained at 25 °C. This study also confirmed an altered circadian rhythm in pathological *Drosophila* compared to non-pathological *Drosophila* aged 2-3 days and maintained at 25 °C. There was no change in

metabolism in the pathological or non-pathological *Drosophila* melanogaster that had been aged five days and 14 days respectively when *Drosophila* were maintained at 25 °C or 29 °C. Collectively, the data from the behavioral proofs of concept generated by this study provided valuable baseline data that future research may be based upon.

Acknowledgments

To Dr. Marla Tipping, Dr. Elisabeth Arevalo, Dr. Pamela Snodgrass, Dr. James Waters, Dr. Brett Pellock, Dr. James Morris, Gail Dourian, the inimitable Trudi Goldberg Pires, Rachel Gregorek, Dr. Daniel Mongeon, Dr. Stephen Blinn, the undergraduates in the Tipping Lab, and countless others from whom I sought advice and guidance along the way: I would like to express my immense and sincere gratitude for the support, encouragement, and guidance I received while working on this research project.

Table of Contents

List of Tables

List of Figures

Chapter I

Introduction

Frontotemporal Dementia

Frontotemporal Dementia (FTD) is a neurodegenerative disease affecting the frontal and temporal lobes of the brain. FTD may be familial or *de novo*, affecting both males and females. There are three variants of FTD: Primary Progressive Aphasia and Movement Disorders, and Behavioral variant (bvFTD) (National Institute on Aging, 2023). Individuals with bvFTD variant exhibit symptoms that include changes in behavior, circadian rhythm, and metabolism. Onset of symptoms begins between ages 27-83 (Balendra & Isaacs, 2018). Given the wide range of symptoms, obtaining a correct diagnosis can prove to be daunting and financially exhausting, as the symptoms overlap with many other known dementias and mental health disorders. Currently, there is no known cure for FTD (Yang et al., 2020).

C9ORF72, Dipeptide Repeats, *GAL4*-UAS System, and FTD

In 2011, the Chromosome 9 Open Reading Frame 72 (*C9ORF72*) protein was discovered. Since that time, *C9ORF72* has become widely recognized as the most common genetic cause for FTD, with 25% of familial cases being attributed to the *C9ORF72* mutation (Smeyers et al., 2021). Research efforts have shown hexanucleotide expansion repeats in the first intron of *C9ORF72* contribute to FTD pathology (Smeyers et al., 2021) (Figure 1). A normal expansion has between two and 24 repeats per *C9ORF72* allele. The pathological expansion repeat range has any number of repeats

greater than 30 per *C9ORF72* allele, but often this number can be in the thousands (Smeyers et al., 2021; Wang et al., 2015). Though *C9ORF72* is highly conserved across many species, there is no homolog in *Drosophila melanogaster* (Smeyers et al., 2021). Therefore, to study *C9ORF72* in *Drosophila* for the research in this project, the *Drosophila* were genetically modified to carry this protein. This was accomplished via the UAS-*GAL4* system.

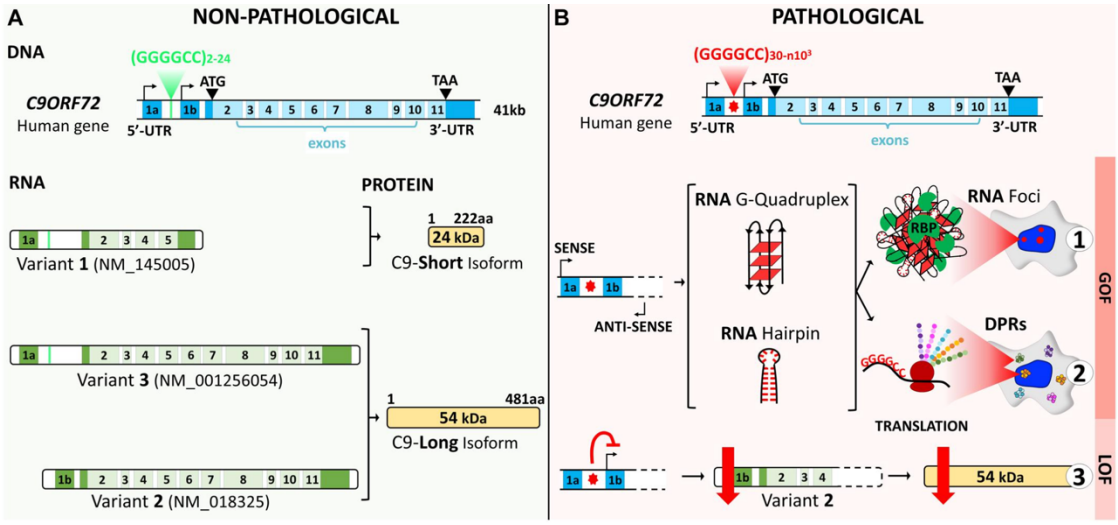

Figure 1. A schematic of *C9ORF72* and dipeptide repeats in non-pathological and pathological conditions (Smeyers et al., 2021).

There are multiple components of the UAS-*GAL4* system that are used to generate a genetic cross. In the first line, or responder line, there is an upstream activation sequence (UAS) (Figure 2). The UAS controls the target gene of interest, but the responder line does not contain the transcriptional activator (Brand & Perrimon, 1993). The transcriptional activator is a yeast protein named *GAL4*. *GAL4* is needed to activate

the target gene, which for the purpose of our research, is *C9ORF72*. *GAL4* is under the influence of the embryonic lethal abnormal visual (*ELAV*) system promoter. The *ELAV* gene is only active in neurons, meaning *C9ORF72* will only be expressed in neuronal tissue when its expression is turned on. In the second line (or, driver line) the *GAL4* transcriptional activator is present but the target gene, *C9ORF72*, is not present (Brand & Perrimon, 1993). When the driver line is crossed with the responder line the following sequence of events takes place: Under the direction of the *ELAV* promoter, the *GAL4* transcription activator acts on UAS to drive overexpression of *C9ORF72*. As a result, UAS subsequently turns on the expression of *C9ORF72* only in neuronal tissue of the resulting progeny (Brand & Perrimon, 1993). This allowed for investigation of the *C9ORF72* phenotype that would otherwise not have been present in *Drosophila*. Furthermore, this study utilized the *C9ORF72* gene construct created by Goodman & Bonini (2019). This construct was designed to only have the first non-coding exon which contained a leader sequence (LDS) and hexanucleotide repeat expansions. This allowed for the investigation of the hexanucleotide repeat expansions specifically rather than the entire *C9ORF72* gene (Goodman & Bonini, 2019).

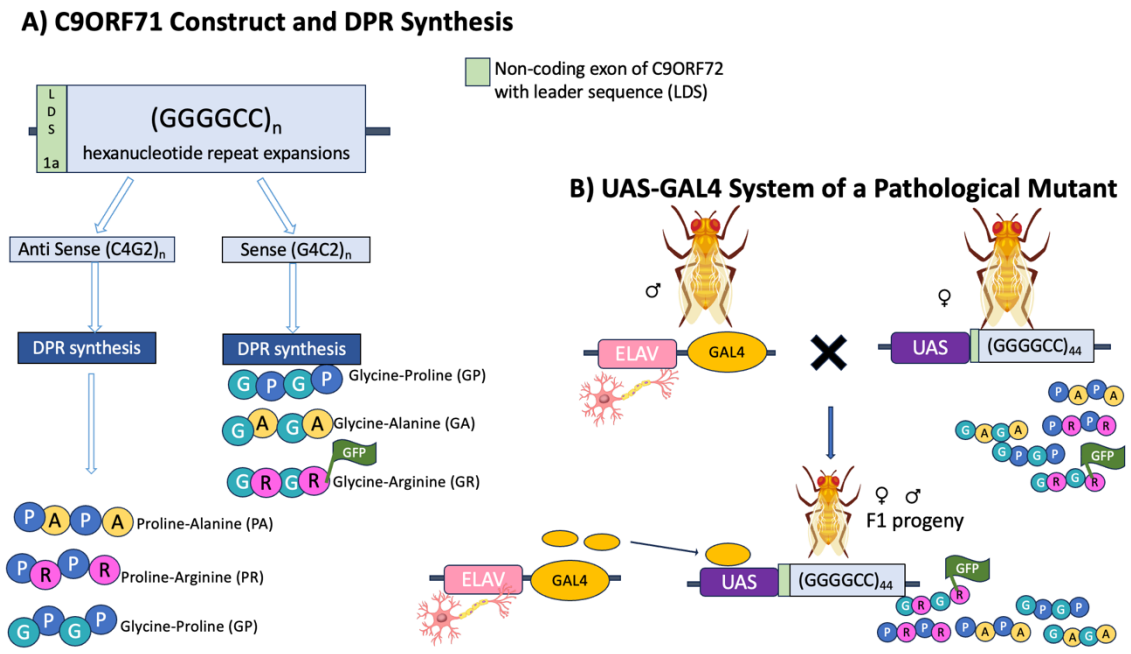

Figure 2. Schematic of *C9ORF72* gene sequence UAS-*GAL4* System. Image created by Nicodemus (2024) based on images found in Balendra & Isaacs, 2018, Brand & Perrimon, 1993, and Braems et al., 2020.

(A) The truncated C9ORF72 gene shown with the coding exons non-coding exon (light green) that contains a leader sequence (LDS). The hexanucleotide repeat expansions give rise to five dipeptide repeats (DPRs). Three anti sense strand DPRs Proline-Alanine (PA), Proline-Arginine (PR), and Glycine-Proline (GP) are generated, as are three sense strands: Glycine-Proline (GP), Glycine-Alanine (GA), and Glycine-Arginine (GR). For the purpose of this research, the GR DPR has been tagged with green fluorescent protein (GFP). (B) A schematic example of a pathological mutant generated via the UAS-GAL4 system. A male Drosophila with an ELAV promoter and a GAL4 transcription activator is crossed with a female Drosophila that has a UAS, target gene of interest, C9ORF72 and five DPRs including a GFP-tagged GR DPR. The cross gives rise to male and female progeny that have an ELAV promoter that directs GAL4 to act on UAS to activate overexpression of C9ORF72 and DPR synthesis.

C9ORF72 contributes to FTD pathology via three mechanisms. The first mechanism is a loss of function of *C9ORF72*, whereby the hexanucleotide repeat expansions cause a decrease in messenger ribonucleic acid (mRNA) levels of *C9ORF72*,

leading to a decrease in the expression of *C9ORF72*. The second mechanism is a gain of function of *C9ORF72*. In this mechanism, due to the hexanucleotide repeats expansions of *C9ORF72*, the formation of G-quadruplexes and R-loops occurs (Smeyers et al., 2021). G-quadruplexes are guanine rich single stranded deoxyribonucleic acid (DNA) structures containing hairpins and tetrads (Wang, et al., 2015). G-quadruplexes function to stabilize the formation of R-loops. R-loops is a term referring to the hybridization of ribonucleic acid (RNA) and DNA (Wang et al., 2021). R-loops have been implicated in transcription dysregulation and in regulating methylation of histones and deoxyribonucleic acid (DNA) (Wang et al., 2015). The third mechanism, which is the focus of this research project, is the generation of pathological dipeptide repeats (DPRs) (Smeyers et al., 2021).

C9ORF72 induced DPR pathology has been found to occur in the neurons and glia of patients with FTD. Specifically, the DPRs form inclusions that accumulate in the neurons and glia. There are five DPRs are synthesized during Repeat associated non-AUG (RAN) translation of *C9ORF72* hexanucleotide repeat expansion (Figure 2). The DPR of interest for this project is the glycine arginine (GR) DPR translated from the sense strand during RAN translation (Freibaum & Taylor, 2017). GR DPRs are highly charged, polar, and toxic in neuronal tissue. GR DPRs localize to the nucleolus, altering ribosomal RNA synthesis. GR DPRs have also been shown to localize to the cytoplasm. Once there, GR DPRS have implicated in the disruption of stress granules, which protect cells from damage during cellular stress (Freibaum & Taylor, 2017; Baradaran-Heravi et al., 2019). Though the understanding of the GR DPRs has become more lucid, further

research needs to be conducted to better understand the mechanism underlying GR DPR neurotoxicity.

C9ORF72, Glucose Metabolism, and FTD

Mechanistically, glucose is broken down via glycolysis, an anaerobic process required for normal cellular metabolism. Glycolysis results in synthesis and release of adenosine triphosphate (ATP). ATP is the energy source used by many cells in the body to perform critical cellular functions. (Hantzidiamantis et al., 2022). The human brain requires an estimated 20% of the total available energy generated by glycolysis. Decreased levels of glucose have a detrimental impact on normal cellular function and survival of brain cells. Patients with FTD experience glucose hypometabolism, or a decrease in the breakdown of glucose, which results in a decrease in ATP synthesis and release. Specifically in behavioral variant FTD, glucose hypometabolism was found to occur in the frontal and temporal lobes. The disruption in glucose metabolism is partly attributed to *C9ORF72* (Garrett & Niccoli, 2022).

In patients with amyotrophic lateral sclerosis (ALS) and who have *C9ORF72* hexanucleotide repeat expansions, it was shown that glucose metabolism is decreased by nearly 50% in their motor neurons (Garrett & Niccoli, 2022). In a study using *Drosophila* modeling ALS with 36 *C9ORF72* hexanucleotide repeat expansions, Atilano et al. (2021) discovered insulin signaling was decreased. Insulin signaling is necessary for regulation of glucose metabolism (Boucher et al., 2014). Atilano et al (2021) also determined overexpression of a *Drosophila* insulin/insulin like growth factor receptor reduced GR DPR toxicity. This same study also demonstrated administration of insulin significantly

increased the survival rate of Drosophila (Atilano et al., 2021). In human patients with FTD, glucose metabolism was measured via a 18F-FDG positron emission test. In this study, patients had a significantly decrease in glucose metabolism compared to their baseline values and to the control subjects (Diehl-Schmid et al., 2007). Very few studies have focused on the relationship between glucose metabolism and FTD. More research is needed to elucidate the role that *C9ORF72* hexanucleotide repeat expansions and GR DPRs play in glucose hypometabolism.

XFe96 Metabolic Analyzer

The Agilent XFe96 Metabolic Analyzer (XFe96) allows researchers to obtain two measurements to assess basal metabolism for the purpose of studying energy usage by a cell in real time. Energy is primarily generated via two mechanisms: (1) mitochondrial respiration and (2) glycolysis, a process in which glucose is converted into lactate (Agilent Technologies, 2023a). There are four ways to classify the bioenergetic phenotype of a cell. The quiescent phenotype is used to classify a cell that is not very energetic in mitochondrial respiration or in glycolysis. The energetic phenotype is used to classify a cell that is using both mitochondrial respiration and glycolysis. The aerobic phenotype is used to classify a cell that primarily uses mitochondrial respiration. Lastly, the glycolytic phenotype is used to classify a cell that primarily uses glycolysis (Agilent Technologies, 2023b).

The first measurement is taken via fluorophores that detect oxygen consumption rate (OCR). OCR measures the capacity a cell has to consume oxygen via mitochondrial respiration by assessing the change in concentration of oxygen over time (Agilent

Technologies, 2023a). The second measurement, extracellular acidification rate (ECAR), is taken via a fluorophore that senses changes in hydrogen proton levels that occur during glycolysis. During glycolysis, hydrogen protons are released. The release of hydrogen protons causes the solution to become more acidic, resulting in a detectable change in pH of the solution. Thus, ECAR measurement reflects a tissue's ability to undergo glycolytic respiration by detecting changes in hydrogen proton levels in real time. (Agilent Technologies, 2023a). The XFe96 also allows for assessment of tissue in response to drugs, such as inhibitors, activators, and substrates to further elucidate the function of the sample tissue (Agilent Technologies, 2023a).

Prior to the development of a clever new protocol by Neville et al. (2018) that may be used when running a metabolic assay, measuring whole brain basal metabolism or even metabolism of specific tissue of small animal models in a non-invasive manner was exceedingly difficult. The difficulty arose when a researcher needed to measure metabolism of a small tissue sample with a non-uniform shape, such as a brain. Rather than remaining immobile at the base of the well, the sample of interest moved around in the well when the measurement probe was lowered down into and raised up out of the solution in the well. The movement of the sample impaired a researcher's ability to achieve accurate and reproducible results. The new protocol uses a micro-tissue restraint to ensure the tissue of interest remains in one place while the probe take measurements (Neville et al., 2018). This design has ushered in an exciting new method of neurometabolic research.

To date, scant few neurodegenerative studies investigating tissue samples from *Drosophila* modeling FTD have been conducted. Using the XFe96, Lai et al. (2023)

assessed metabolic change in adult *Drosophila* in response to manganese induced Parkinson's disease. The researchers determined manganese lowered OCR and the changed the bioenergetic phenotype from energetic to quiescent (Lai et al., 2023). In a different study also focused on Parkinson's disease pathology, Sarkar et al. (2020) used a *Drosophila* animal model to assess alpha synuclein (α synuclein) with a knockdown model of GTP cyclohydrolase (*Gch1*). *Gch1* regulates α synuclein neurotoxicity in neuronal tissue. Using this knockdown model, they determined that OCR decreased. The model also demonstrated a quiescent bioenergetic phenotype (Sarkar et al., 2020). Given the limited number of longitudinal studies performed utilizing the XFe96 to explore metabolic changes in FTD in small animals, it is reasonable to assert that more research should be pursued to better understand the nexus of metabolism and FTD.

Circadian Rhythm, Behavioral Monitoring, and FTD

Sleep cycles change with age, with a decline in total sleep duration increasing as a person ages. The decrease in sleep has a negative impact on cognition and metabolism (Mattis & Sehgal, 2017). Oscillation of the day and night circadian rhythm is tightly regulated via the suprachiasmatic nucleus (SCN). The primary SCN is located in the anterior hypothalamus region of the brain (Carter et al., 2021). In humans, a transcription factors named Brain and muscle arnt-like (*BMAL1*) forms a heterodimer complex with another transcription factor, circadian locomotor output cycles kaput (*CLOCK*) (Figure 3) (Abe et al., 2022). Early in the day cycle of circadian rhythm, this *BMAL1*/*CLOCK* heterodimer is capable of initiating transcription of two genes, Period (*Per*) and Cryptochrome (*Cry*). Early in the night cycle of circadian rhythm, *Per* and *Cry* form a complex which in turn can suppress activity of the *BMAL1*/*CLOCK* heterodimer, setting

up a negative feedback loop. The negative feedback action exerted by the *Per*/*Cry* heterodimer on the *BMAL1*/*CLOCK* heterodimer subsequently elicits a reduction on transcription of *Per* and *Cry* and reduces the negative feedback on the *BMAL1*/*CLOCK* heterodimer. It is this reduction in negative feedback on the *BMAL1*/*CLOCK* heterodimer that allows for the start of a day cycle again (Mattis & Sehgal, 2017).

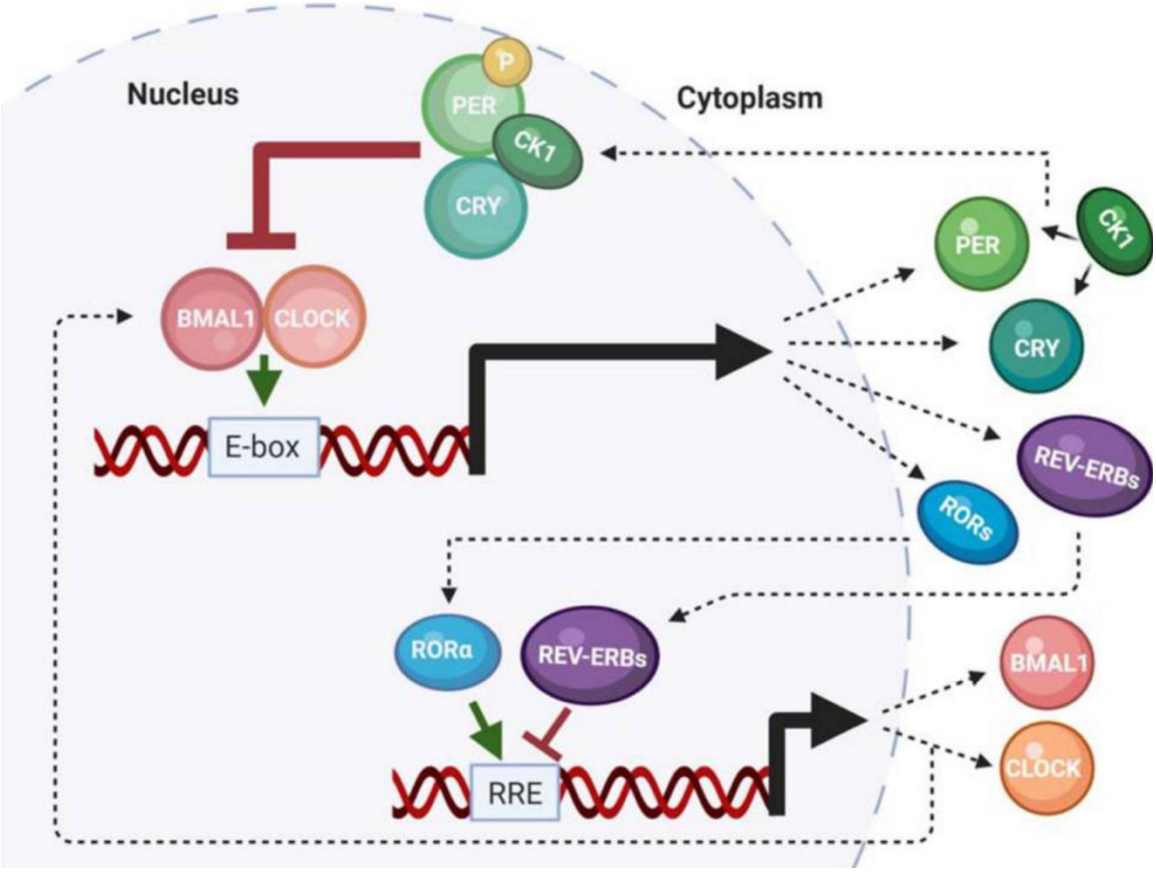

Figure 3. Visual of molecular circadian clock (Carter, et al. 2019).

Depiction of negative feedback loops that regulate circadian rhythm.

Environmental factors, such as light, can influence the function of the SCN. Retinal ganglion cells are sensitive to light. Light is absorbed by the retinal ganglion

cells. The retinal ganglion cells send a signal to the SCN to suppress the production of melatonin by the pineal gland and initiating the circadian rhythm day cycle. Light exposure that falls outside of the normal day and light cycle suppresses melatonin production, resulting in disrupted sleep (Figure 4) (Carter et al., 2021; Dedeene et al., 2019).

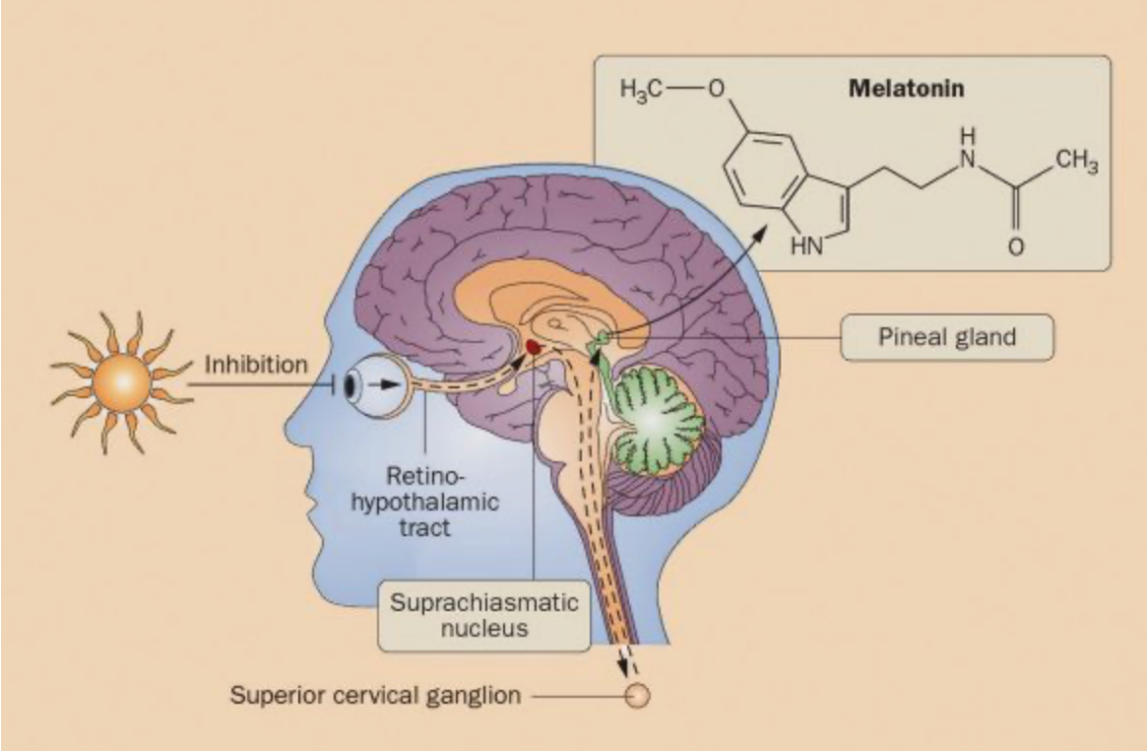

Figure 4. Visualization of suprachiasmatic nucleus and pineal gland (American Chemical Society, 2023).

A source of light initiates signaling which reaches the SCN, leading to suppression of melatonin synthesis by the pineal gland.

Through the use of sleep diaries and a wearable sensor contained in a wristwatch-like device known as an actigraph unit, it has been reported that FTD patients have significant sleep disturbances. Specifically, there is an increase in activity during the night and a decrease in activity in the morning (Anderson et al., 2009). In lieu of an actigraph to monitor the sleep cycle of *Drosophila*, the DAM5H behavioral monitor allows for real time monitoring of movement of *Drosophila* over a period of time, representing an ideal non-intrusive method for studying sleep cycles in *Drosophila* (Trikinetics USA, 2023).

Previous research has shown significant GR DPR inclusions were found in the pineal gland cells of FTD patients with *C9ORF72* hexanucleotide repeat expansions upon post-mortem examination (Dedeene et al., 2019). While limited studies exist with respect to circadian rhythm and FTD in humans, *Drosophila* have been used to investigate various aspects of circadian rhythm. For example, loss of *Per* expression in *Drosophila* was shown to expedite the neurodegeneration process via increased oxidative damage and reduced capacity to respond to stress. Moreover, *Drosophila* have also been shown to exhibit loss of circadian rhythm with age (Carter et al., 2019). Minimal research has been conducted to monitor sleep wake cycles in *Drosophila* with an overexpression of *C9ORF72*.

Drosophila melanogaster and FTD

When Thomas Hunt Morgan proved the chromosome theory using the *Drosophila* animal model in 1910, other genetic researchers were keen to recognize that Morgan was onto a winner (Miko, 2008). Indeed, in the years that followed, *Drosophila* became the

darling of the genetic research world. In general, *Drosophila* are perceived as an ideal research model owing to a minimal space requirement for stock and cross maintenance, are relatively inexpensive to keep, are capable of rapid reproduction, produce a yield high volume of progeny, are genetically modifiable, and have average lifespans of roughly 70 days which makes them suitable for longitudinal studies (Tolwinski, 2017; Piper & Patridge, 2018). Additionally, *Drosophila* are ectotherms*,* meaning they respond to changes in environmental temperature. Maintaining *Drosophila* at different temperatures allows for the study of normal and severe disease phenotypes (Jakšić & Schlötterer, 2016).

Temperature differences elicit changes physiologic processes, such as gene expression and changes in behavior. Previous studies using *Drosophila* have demonstrated that genes are significantly altered due to temperature changes. This change is known as phenotypic plasticity. Per Jakšić & Schlötterer (2016), phenotypic plasticity is defined as the ability of a given phenotype to display a range of phenotypes as a response to environmental heterogeneity (Jakšić & Schlötterer, 2016). In a study conducted by Molón et al. (2020), a higher temperature of 28°C hastened the metabolism and aging in both male and female *Drosophila (*Molón et al., 2020). Additionally, a separate study found *Drosophila* with 160 *C9ORF72* hexanucleotide repeat expansions maintained at 29°C exhibited a four-fold higher synthesis of DPRs when compared to *Drosophila* maintained at 25°C (Tran et al., 2015). Of significance is that in Drosophila, the activity of *GAL4* is temperature dependent. Specifically, an increase in temperature results in an increase in *GAL4* activity. Subsequently, UAS activation increases, resulting in an increase in the expression of the target gene. A temperature of 29 °C is considered

the maximal temperature for *GAL4* activity (Duffy, 2022). Therefore, is it reasonable to question whether a severe metabolic phenotype, a severe circadian rhythm phenotype, and expedited aging would be observed in pathological *Drosophila* with 44 hexanucleotide repeat expansions modeling FTD and maintained at 29°C but would not be observed in non-pathological *Drosophila* with 12 hexanucleotide repeat expansions modeling FTD and maintained at 29°C.

Research Aims, Goals, and Hypotheses

The primary focus of this research was to establish two proofs of concepts for circadian rhythm and metabolism in Frontotemporal Dementia (FTD) using a *Drosophila melanogaster* animal model that had been genetically modified to have an overexpression of the Chromosome 9 Open Reading Frame 72 protein (*C9ORF72*). Based upon on the circadian rhythm and metabolism literature reviews, we hypothesized an overexpression of *C9ORF72* protein in a *Drosophila melanogaster* model would lead to a change in circadian rhythm and metabolism. More specifically, the pathological group with 44 hexanucleotide repeat expansions representing would correlate with a significant change in circadian rhythm and metabolism in aged *Drosophila melanogaster* whereas the non-pathological group with 12 hexanucleotide repeat expansions would not correlate with a significant change in circadian rhythm or metabolism. Testing this hypothesis required two specific aims which were derived from the primary objective.

Primary objective:

Demonstrate a change in circadian rhythm and metabolism in an *in vivo Drosophila melanogaster* animal model of FTD and correlate the change in circadian rhythm and

metabolism over time with the number of pathological and non-pathological number of *C9ORF72* hexanucleotide repeat expansions.

Specific Aim 1:

Demonstrate a change in circadian rhythm by using a *Drosophila melanogaster* animal model to model FTD.

Method:

Use a DAM5H behavioral monitor to total the number of movements, or counts, each fly took over the span of three days.

Expected results:

Circadian rhythm would be altered in pathological male and female *Drosophila melanogaster* aged 1 day and maintained at 25°C. Circadian rhythm would not be altered in non-pathological male and female *Drosophila melanogaster* aged 1 day and maintained at 25°C. Circadian rhythm would not be altered in non-pathological male and female *Drosophila melanogaster* aged 2-3 days and maintained at 25°C. Circadian rhythm would be altered in pathological male and female *Drosophila melanogaster* aged 2-3 days and maintained at 25°C.

Specific Aim 2:

Demonstrate a change in metabolism by using a *Drosophila melanogaster* animal model to model FTD.

Method:

Use a XFe96 Metabolic Analyzer to measure oxygen consumption rate and extracellular acidification rate to assess a change in metabolism.

Expected results:

Metabolism would not be altered in non-pathological or pathological male and female *Drosophila melanogaster* aged five days and maintained at 25°C. Metabolism would not be altered in non-pathological male and female *Drosophila melanogaster* but would be altered in pathological male and female *Drosophila melanogaster* aged 14 days and maintained at 25°C.

Metabolism would not be altered in non-pathological or pathological male and female *Drosophila melanogaster* aged five days and maintained at 29°C. Metabolism would not be altered in non-pathological male and female *Drosophila melanogaster* but would be altered in pathological male and female *Drosophila melanogaster* aged 14 days and maintained at 29°C.

Chapter II

Methods

The following information describes the methods pertaining to the assays used to conduct the research as well as methods used with respect to *Drosophila.*

Animals

Drosophila melanogaster were maintained at 25 °C and 29 °C on a molasses food medium in polystyrene vials with cotton plugs. *Drosophila* stocks 8765, 84722, and 84723 were obtained from Bloomington Drosophila Stock Center (BDSC) (Table 1). The 84722 and 84723 lines contained the *C9ORF72* construct previously discussed. The severe *GAL4-ELAV* line was obtained from Alexey Veraksa's lab at University of Massachusetts Boston (Table 1). *Drosophila* stocks were flipped once per month. Genetic crosses were flipped every three to four days.

Table 1. *Drosophila* stock list: Table with stock number, genotype, and classification. *Drosophila melanogaster* stock obtained from Bloomington Drosophila Stock Center.

Stock #	Genotype	Classification
8765	P{w[+mC]=*GAL4-ELAV*.L}2/CyO	Driver Line
84722	P{w[+mC]=UAS-LDS-(G4C2)12.GR-GFP}2	Non-pathological mutant control line
84723	w[1118]; P{w[+mC]=UAS-LDS-(G4C2)44.GR-GFP}9	Pathological mutant line
Veraksa	*GAL4-ELAV*	Severe Driver Line

To create a pathological genetic cross for use in the XFe96 Metabolic Analyzer assay, a total of 10 female *Drosophila* from the 84723 pathological mutant line were placed into a vial with five male *Drosophila* from the 8765 *GAL4-ELAV* driver line. To create a non-pathological genetic cross, a total of 10 *Drosophila* from the 84722 non-pathological control line were placed into a vial with five male *Drosophila* from the 8765 *GAL4-ELAV* driver line. To create a pathological genetic cross for the DAM5H behavioral assay, a total of 10 female *Drosophila* from the 84723 pathological mutant line were placed into a vial with five male *Drosophila* from the *GAL4-ELAV* driver line. To create a non-pathological genetic cross, a total of 10 *Drosophila* from the 84722 non-pathological control line were placed into a vial with five male *Drosophila* from the *GAL4-ELAV* driver line. After creating genetic crosses for the respective assays, the vials were then placed in a 25 °C incubator or a 29 °C incubator. The *Drosophila* were moved into a new vial every three days. Progeny maintained at 25 °C began to emerge after 10-12 days. Progeny maintained at 29 °C began to emerge after 5-6 days. Every two days, the progeny were collected from the vial and placed into a new vial. Every three days, the progeny were flipped into a new vial. This process was repeated until the progeny reach the desired age (Figure 5). Once the *Drosophila* reached the desired age, they could be used in an assay.

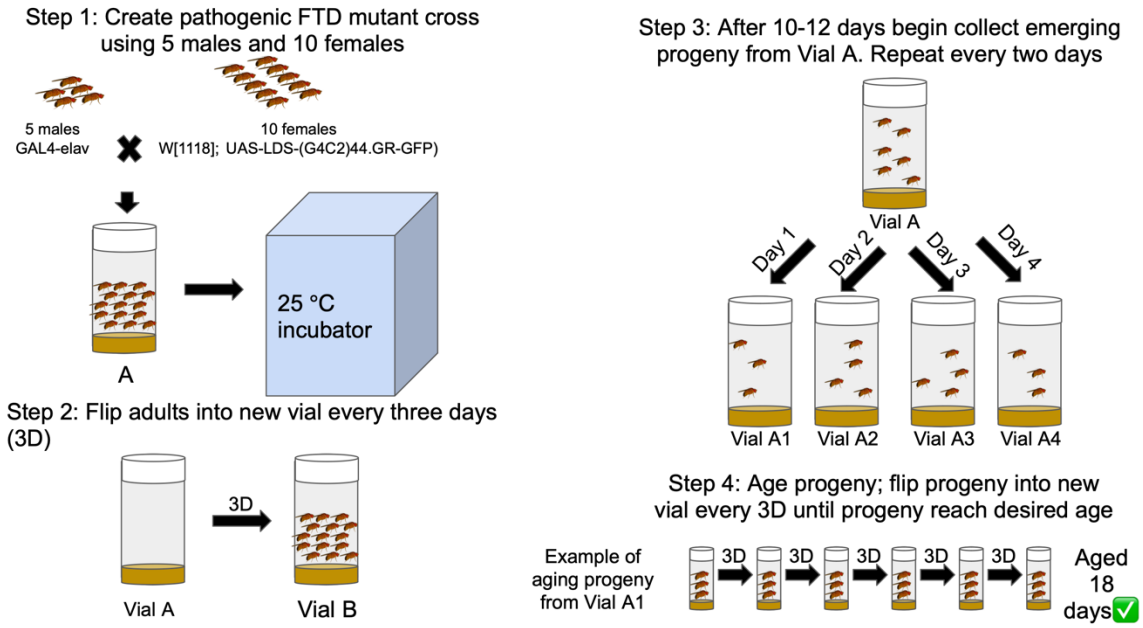

Figure 5. Schematic of setting up genetic cross and aging progeny (Nicodemus, 2023).

Five adult male Drosophila from the driver line are crossed with 10 females form the pathological mutant line. The cross is placed into a vial and the vial is placed in an incubator. The cross is flipped into a new vial every three days. After 10-12 days, the progeny will begin to emerge. Every two days, progeny are collected. Progeny are flipped into a new vial every three days. This is repeated until the progeny reach the target age.

XFe96 Metabolic Analyzer

Briefly, the Agilent XFe96 Metabolic Analyzer (XFe96) was kept in an incubator set to 18°C to prevent the XFe96 from overheating. The XFe96 was set to 25°C with the heat on and was run with Wave software version 2.4. An Agilent XFe96 cartridge (Agilent, 102416-100) was hydrated with 200 µl of calibrant solution (Agilent, 100840-000) at 25°C. Hydration of the cartridge occurred at least two hours prior to use. Over the span of 30 mins, whole brains were dissected out in ringer solution in a Pyrex nine well glass plate. Upon completion of dissection, one brain per well was placed into an Agilent

96-well cell plate (Agilent, 102416-100) containing 50 µl of Agilent XFe96 assay media (Figure 6). Using a probe, individual brains were sunk to the bottom of each well, taking care to center the brain between the three raised spheres in the center of the well (Figure 7). The tissue restraint was then lowered into the well via forceps. Proper orientation of the tissue restraint necessitates the plastic ring to face towards the brain at the bottom of the well and the nylon screen to face the top or opening of the well. The tissue restraint was carefully pushed down toward the bottom of the well using a probe to ensure would not move or float in the well during the assay. To achieve a desired total of 180 µl assay media per well, 130 µl of assay media was gently added to each well, taking care not to disturb the centered brain (Figure 8). A photo of the cell plate was taken to document the respective brains were still centered prior to placing the cell plate on the tray of the XFe96. The instrument was used as is for typical cell assays with all cycle procedures consisting of one-minute mixing, zero-minutes waiting, and three-minutes measuring. A total of seven cycles were run per assay. A photo of the cell plate was after to document the respective brains were still centered after the assay was complete (Figure 9). Results were analyzed and graphed using Prism (GraphPad).

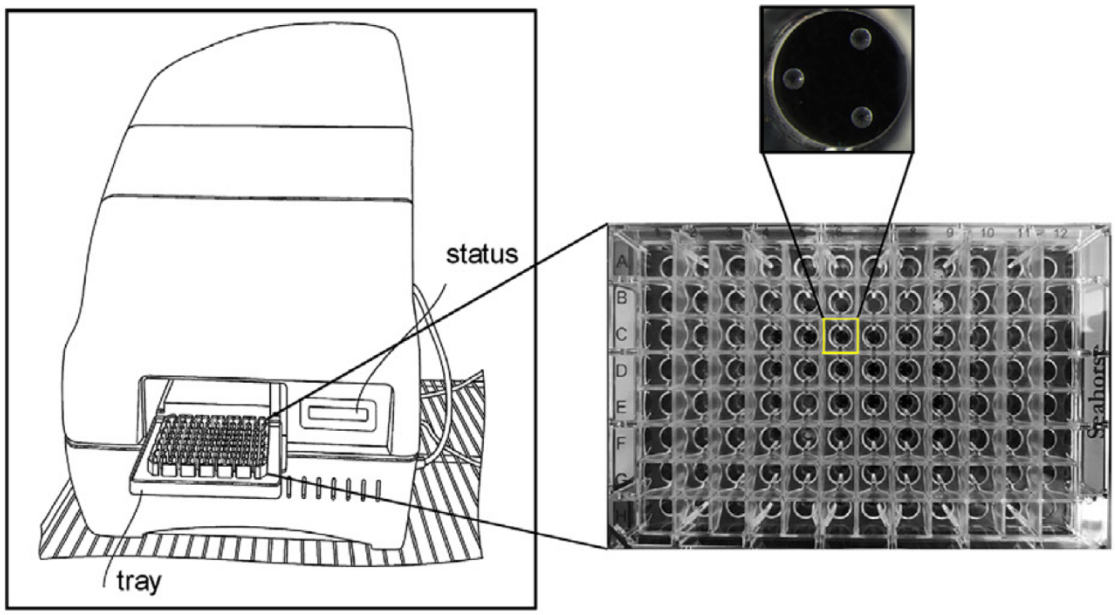

Figure 6. Drawing of XFe96 and well plate (Neville, 2018).

The tray of XFe96 is open to demonstrate how plate is loaded into the XFe96. A single well of a 96 well plate is enlarged to show the three spheres at the bottom of the well that act as a visual guide when centering the brain in the bottom of the well.

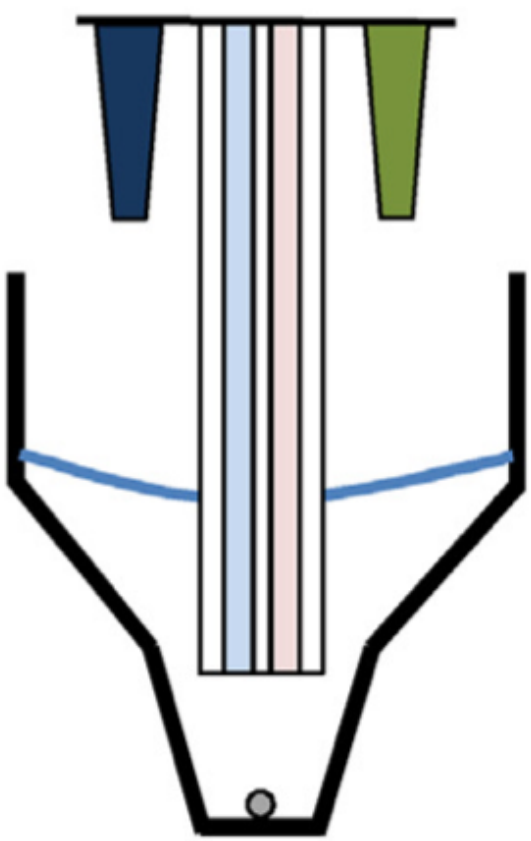

Figure 7. Probe design of XFe96 (Neville, 2018).

Depiction of the probes used to take measurements of oxygen consumption rate (light blue) and extracellular acidification rate (light pink) of tissue (gray circle).

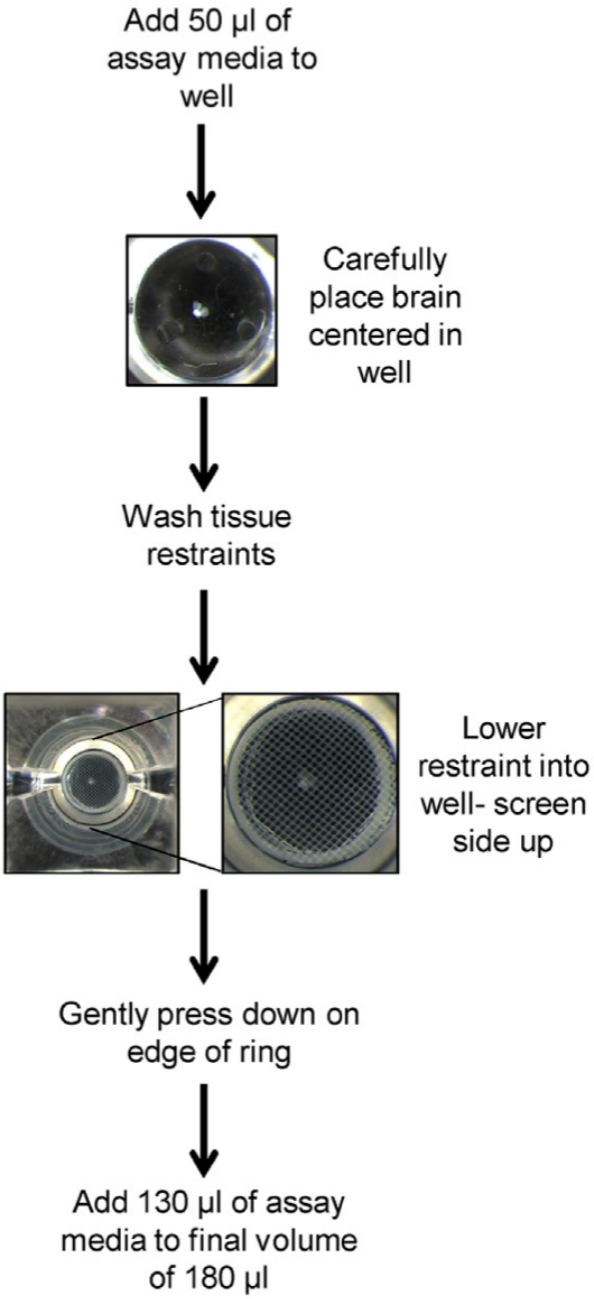

Figure 8. A general schematic workflow of setting up a well (Neville, 2018).

50 µl of media was added to the well and the brain was then placed into the well. The brain was centered, and a washed tissue restraint was positioned into the well so that the screen side of the tissue restraint was facing up. After the tissue restraint was in position, a further 130 µl of XFe96 media was added to the well.

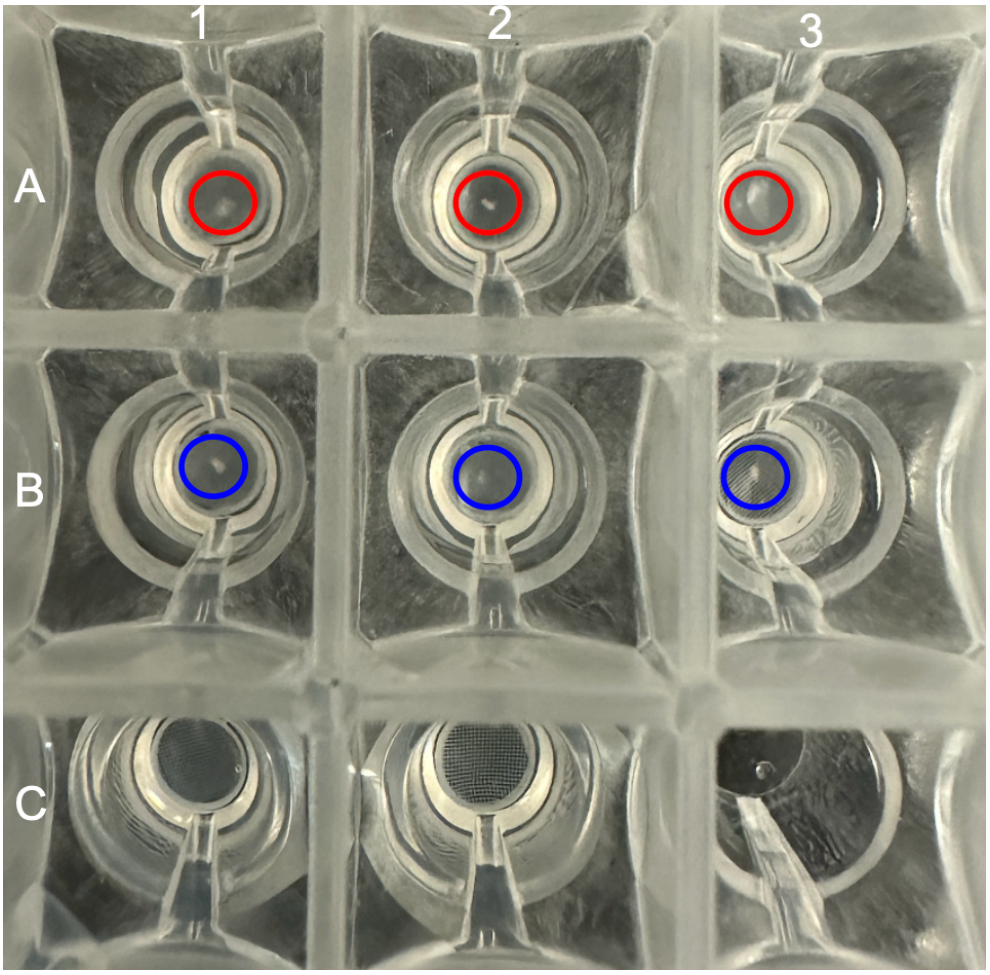

Figure 9. Example of photograph taken after completion of a XFe96 assay (Nicodemus 2023).

Row A1, A2, A3: Red circle around the control brain. Row B1, B2, B3: Blue circle around the pathological brain. Row C1, C2 tissue restraint with no brain in well. Upon visual inspection of the tray following the assay, it is apparent that the control brain in A3 is an example of a brain that is no longer centered post assay. The measurement data for this brain would not be included in data analysis for the run. All other brains remained centered.

DAM5H Behavioral Monitor Assay

To begin setting up the assay, food media was placed in one end of the glass capillary tube. A cap was placed over the end of the tube that had the food media. Repeat this until the number of prepared capillary tubes equals the number of *Drosophila* that

will be used in the assay. Next, on a CO_2 anesthetization pad, briefly anesthetize the desired number of *Drosophila* for each condition that will be used for the assay. Two conditions were tested during each run. For example, if eight male *Drosophila* from the pathological mutant condition were used, then eight male *Drosophila* from the control condition were also be used in the assay. Care was taken to work with one condition at a time to prevent accidentally mixing *Drosophila* from the two conditions. One *Drosophila* was placed into a vial and then a cotton plug was pushed into place at the other end (Figure 10). This set up simulated the vial that the *Drosophila* ordinarily lived in. This capillary tube set up process was repeated as needed until the desired number of *Drosophila* were singularly placed into respective capillary tubes. The behavioral monitor has 32 individual mounts for the capillary tubes, meaning a total of 32 *Drosophila* may be used in an assay (Figure 11). For ease of reading data at the end of the assay, one condition was placed in the odd numbered mounts and the other condition were placed in the even numbered mounts.

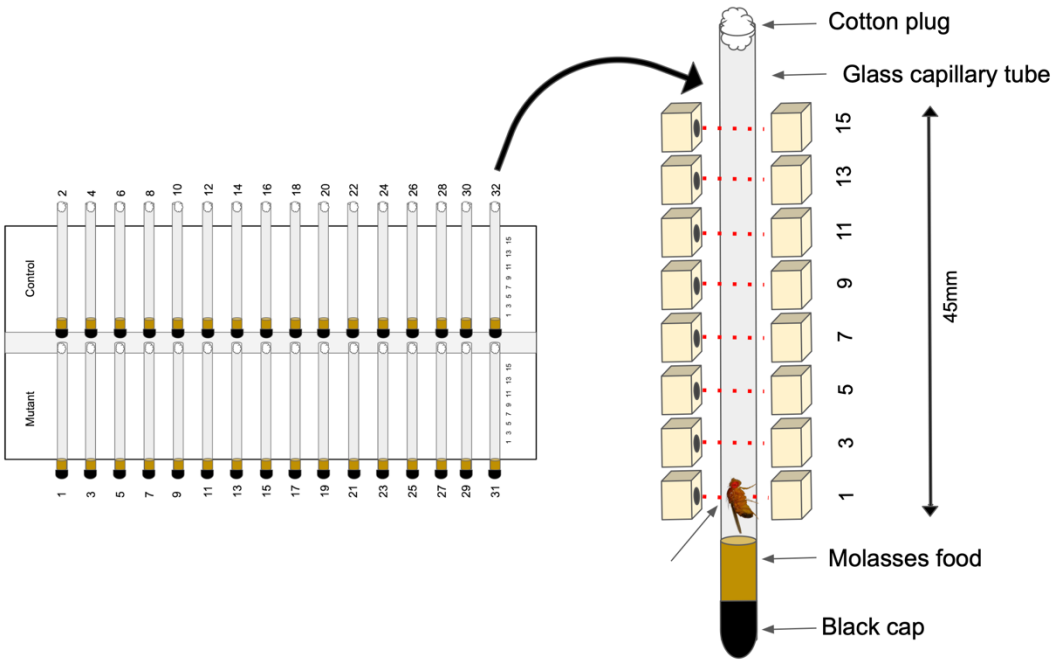

Figure 10. Schematic of a capillary tube set up (Nicodemus, 2023).

An enlarged view of the capillary tube set up depicting one end of the 45 mm capillary tube containing media and a cap. A cotton plug was placed at the other end. The fly was free to move within the capillary tube. If the fly moved in front of the infrared beam, shown as a dashed red line, a count is recorded.

The capillary tube was gently pressed into the mount. After all capillary tubes were pressed into place on the behavioral monitor, the behavioral monitor was placed into an incubator with programmed light cycle of 12 hours of light and 12 hours of darkness. The behavioral monitor is kept in flat, horizontal position. Allowing the *Drosophila* to recover from CO_2 and adjust to the new vial for a couple of minutes was necessary as activity in the initial two minutes of recovery may be frenetic while the *Drosophila* explored their new surroundings. If that activity was recorded, it could possibly skew the data.

While the *Drosophila* were adjusting to the new surroundings, the program software was set up to run an assay. To use the DAM5H Behavioral monitor for a sleep study, the "count" parameter was selected from the software program menu. Counts were registered by each infrared beam when a *Drosophila* crossed in front of the infrared beam (Figure 10). If a *Drosophila* sat in the beam of light, only a single count was recorded. However, if a *Drosophila* moves around in front of the beam, multiple counts would have been recorded. The reading of the count parameter was adjusted so that one reading will be taken every minute. The *Drosophila* remained in the capillary tube for three days to capture activity during a complete sleep cycle. After the assay was over, the *Drosophila* were discarded. The capillary tubes and capillary tube caps were cleaned and allowed to air dry prior to being used again. The cotton plugs were discarded. Results were analyzed and graphed using a Lomb-Scargle Periodogram sinusoidal model.

Figure 11. A photograph of the behavioral monitor set up (Nicodemus, 2023).

32 capillary tubes have been placed into position on the behavioral monitor.

Chapter III

Results

XFe96 Results

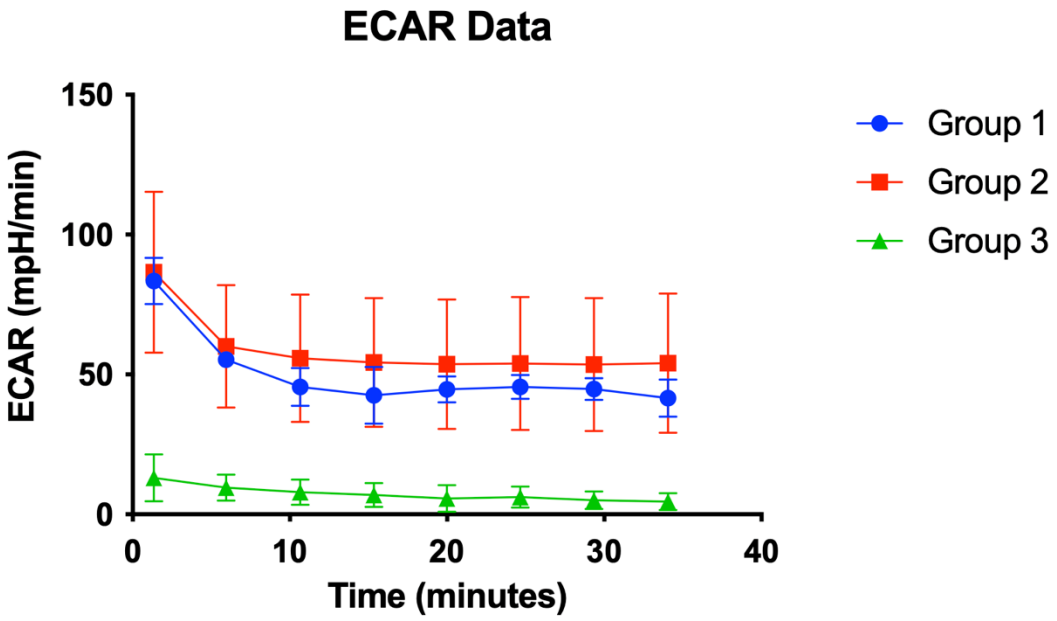

Figure 12. Adult *Drosophila* brain level of extracellular acidification.

Extracellular acidification results of basal level measurement on adult brains of Drosophila aged 5 days in 25 °C. Group 1: UAS-LDS G4C2 (44) pathological mutant brains (blue), n=6. Group 2: UAS-LDS G4C2 (12) non pathological mutant control brains (red), n =6. Group 3: Tissue restraints (green), n=3.

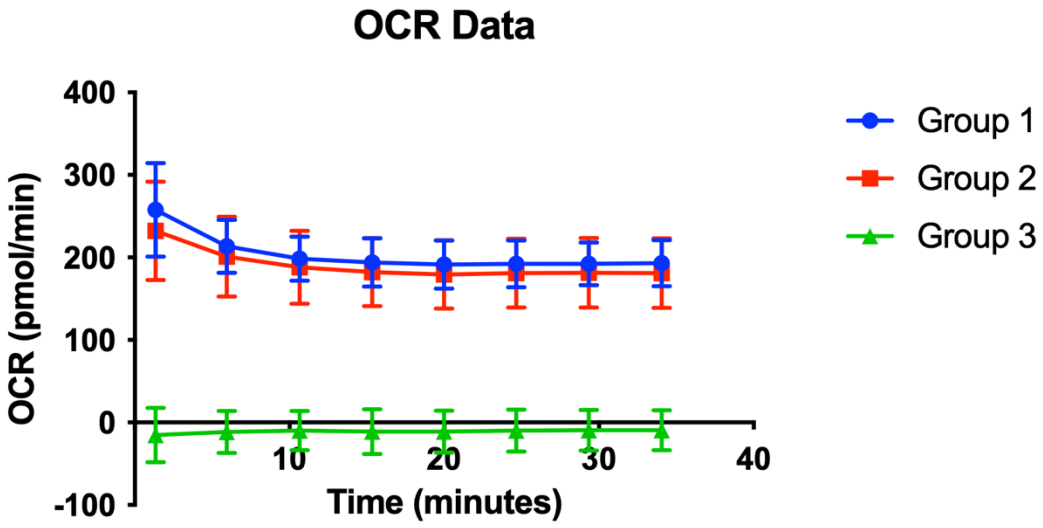

Figure 13. Adult *Drosophila* brain basal level of oxygen consumption rate.

Oxygen consumption rate results of basal level measurement on adult brains of Drosophila aged 5 days in 25 °C. Group 1: UAS-LDS G4C2 (44) pathological mutant brains (blue), n=6. Group 2: UAS-LDS G4C2 (12) non pathological mutant control brains (red), n =6. Group 3: Tissue restraints (green), n=3.

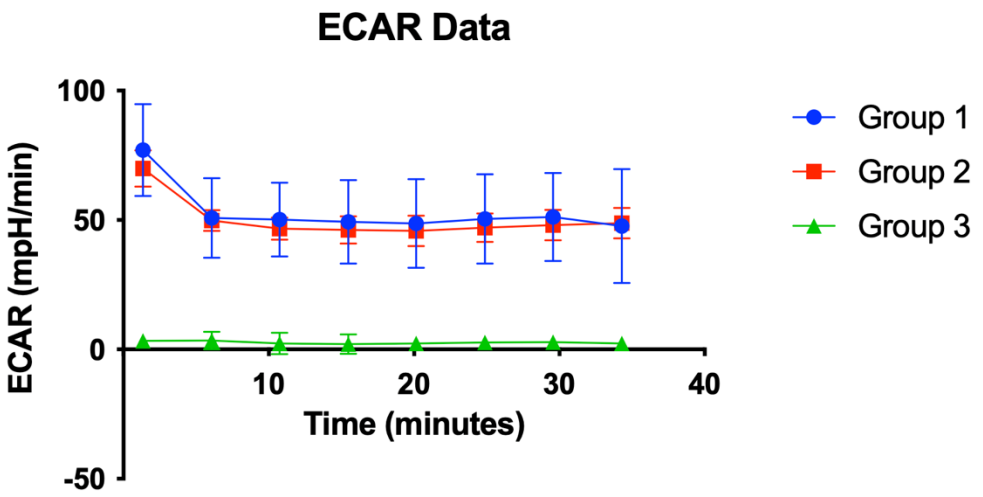

Figure 14. Adult *Drosophila* brain level of extracellular acidification.

Extracellular acidification results of basal level measurement on adult brains of Drosophila aged 14 days in 25 °C. Group 1: UAS-LDS G4C2 (44) pathological mutant brains (blue), n=6. Group 2: UAS-LDS G4C2 (12) non pathological mutant control brains (red), n =5. Group 3: Tissue restraints (green), n=3.

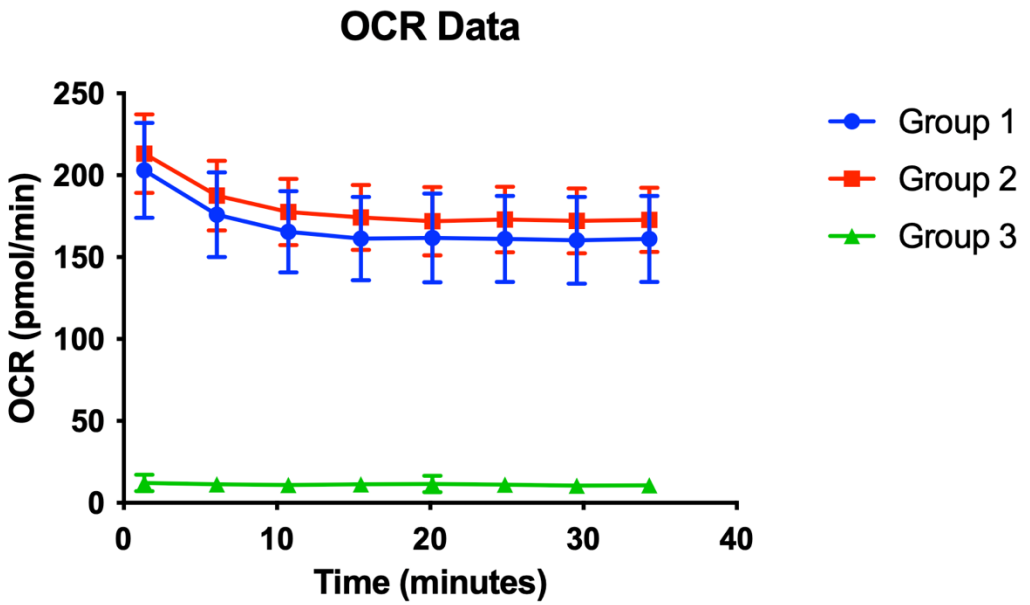

Figure 15. Adult *Drosophila* brain basal level of oxygen consumption rate.

Oxygen consumption rate results of basal level measurement on adult brains of Drosophila aged 14 days in 25 °C. Group 1: UAS-LDS G4C2 (44) pathological mutant brains (blue), n=6. Group 2: UAS-LDS G4C2 (12) non pathological mutant control brains (red), n =5. Group 3: Tissue restraints (green), n=3.

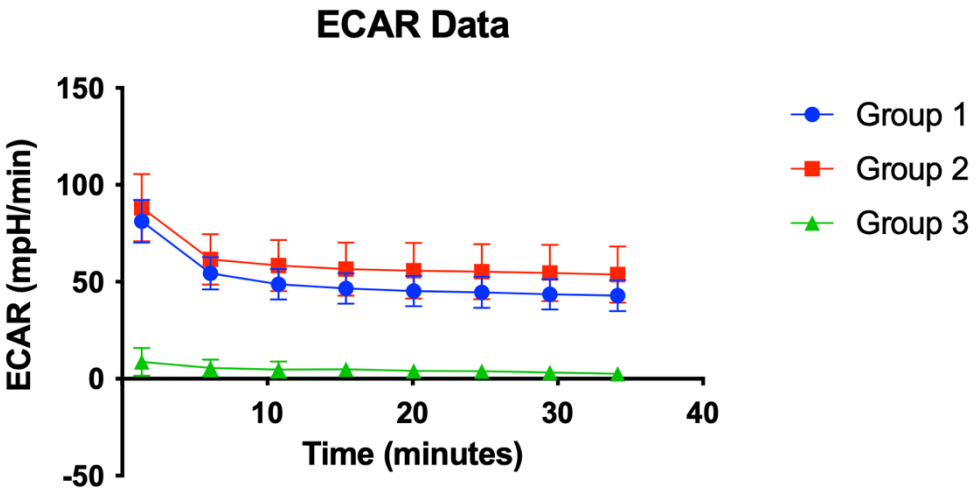

Figure 16. Adult *Drosophila* brain level of extracellular acidification.

Extracellular acidification results of basal level measurement on adult brains of Drosophila aged 5 days in 29 °C. Group 1: UAS-LDS G4C2 (44) pathological mutant brains (blue), n=5. Group 2: UAS-LDS G4C2 (12) non pathological mutant control brains (red), n =6. Group 3: Tissue restraints (green), n=3.

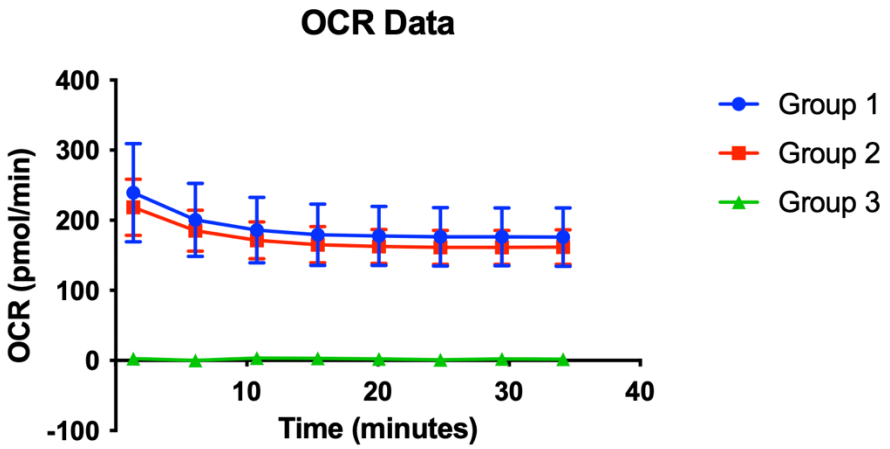

Figure 17. Adult *Drosophila* brain basal level of oxygen consumption rate.

Oxygen consumption rate results of basal level measurement on adult brains of Drosophila aged 5 days in 29 °C. Group 1: UAS-LDS G4C2 (44) pathological mutant brains (blue), n=5. Group 2: UAS-LDS G4C2 (12) non pathological mutant control brains (red), n = 6. Group 3: Tissue restraints (green), n=3.

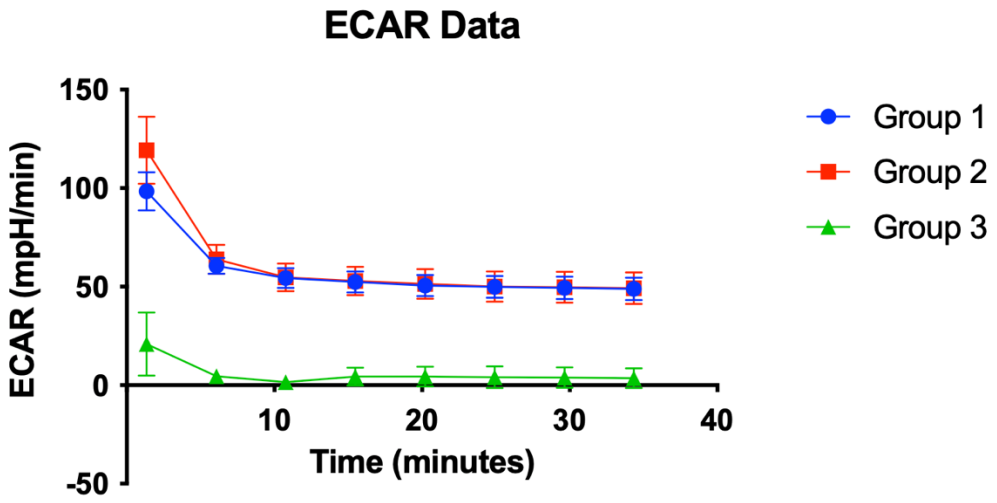

Figure 18. Adult *Drosophila* brain level of extracellular acidification.

Extracellular acidification results of basal level measurement on adult brains of Drosophila aged 14 days in 29 °C. Group 1: UAS-LDS G4C2 (44) pathological mutant brains (blue), n=6. Group 2: UAS-LDS G4C2 (12) non pathological mutant control brains (red), n = 5. Group 3: Tissue restraints (green), n=3.

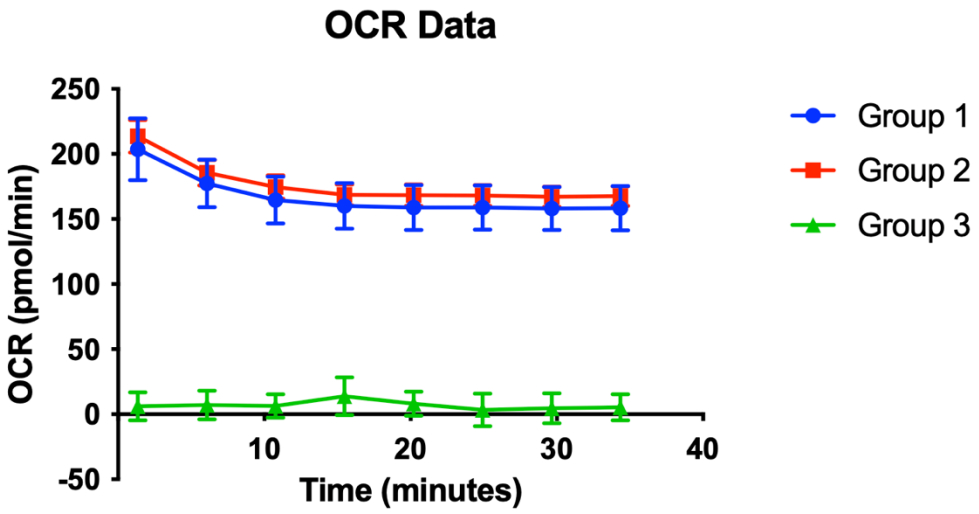

Figure 19. Adult *Drosophila* brain basal level of oxygen consumption rate.

Oxygen consumption rate results of basal level measurement on adult brains Drosophila aged 14 days in 29 °C. Group 1: UAS-LDS G4C2 (44) pathological mutant brains (blue), n=6. Group 2: UAS-LDS G4C2 (12) non pathological mutant control brains (red), n = 5. Group 3: Tissue restraints (green), n=3.

DAM5H Behavioral Monitor Results

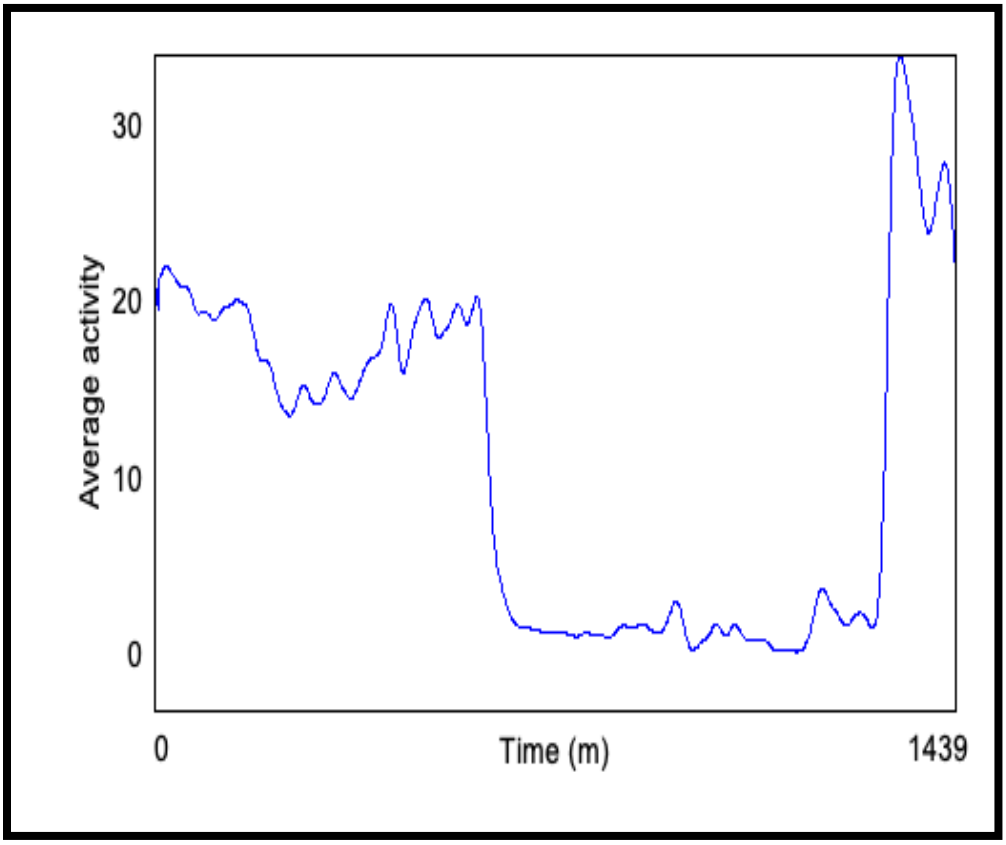

Figure 20. Average activity of non-pathological control *Drosophila* maintained at 25 °C and aged 0-1 days, n=1.

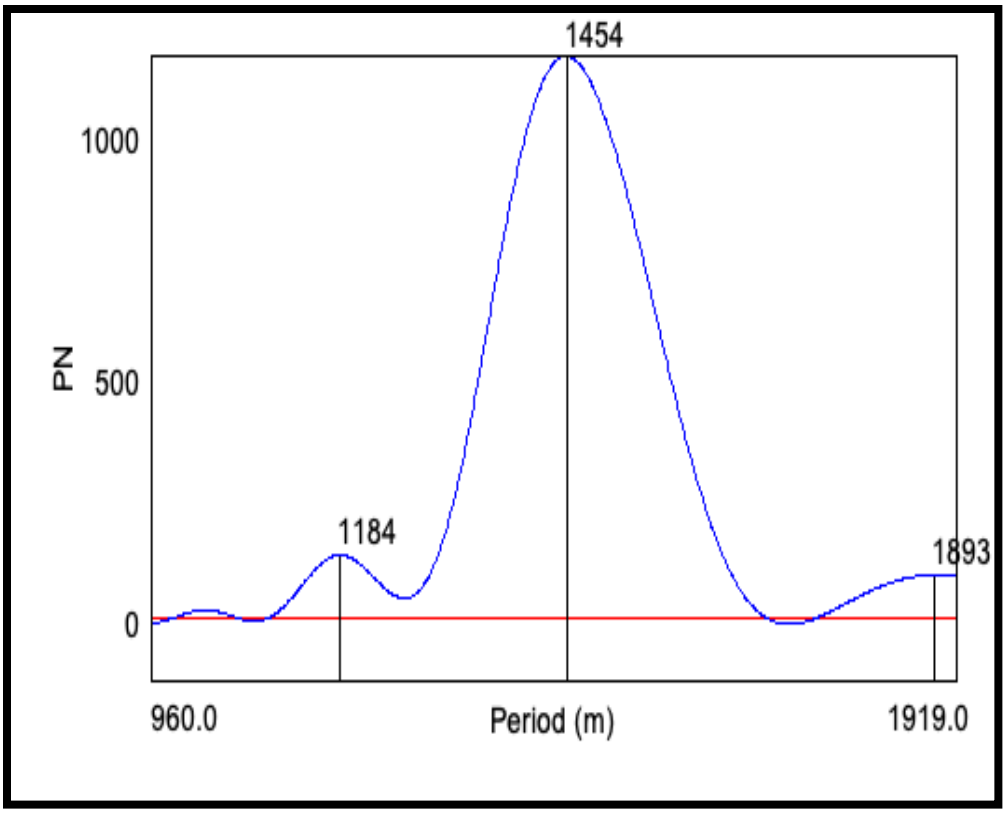

Figure 21. Lomb-Scargle periodogram of non-pathological control *Drosophila* maintained at 25 °C and aged 0-1 days, n=1.

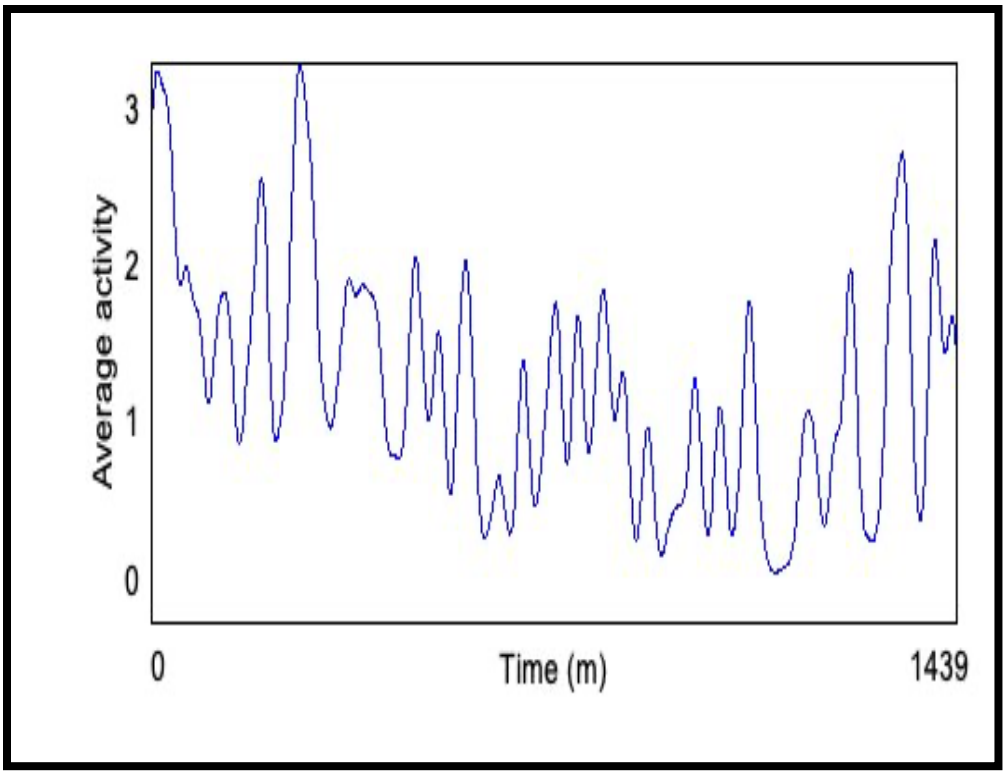

Figure 22. Average activity of pathological mutant *Drosophila* maintained at 25 °C and aged 0-1 days, n=1.

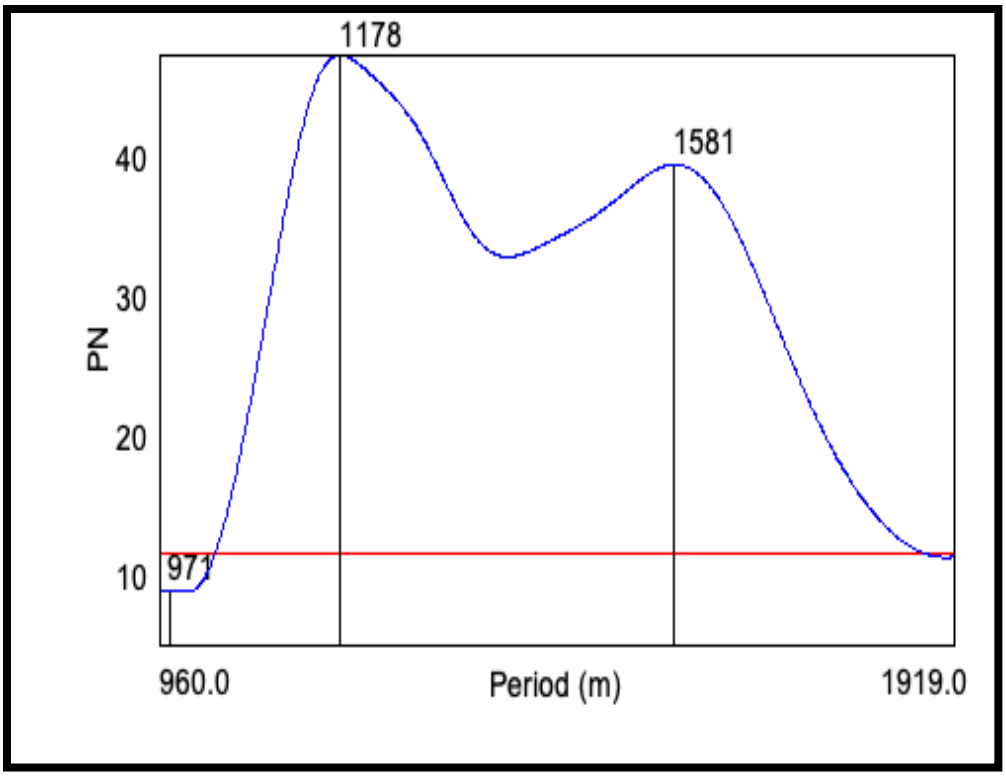

Figure 23. Lomb-Scargle periodogram of pathological mutant *Drosophila* maintained at 25 °C and aged 0-1 days, n=1.

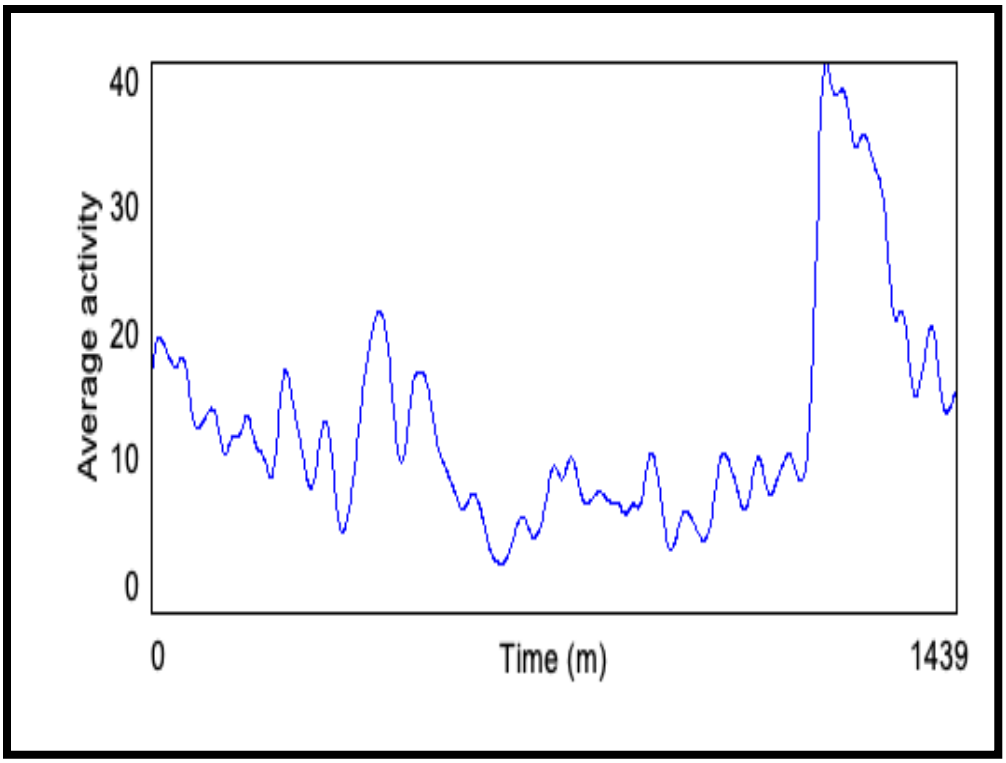

Figure 24. Average activity of non-pathological control *Drosophila* maintained at 25 °C and aged 2-3 days, n=1.

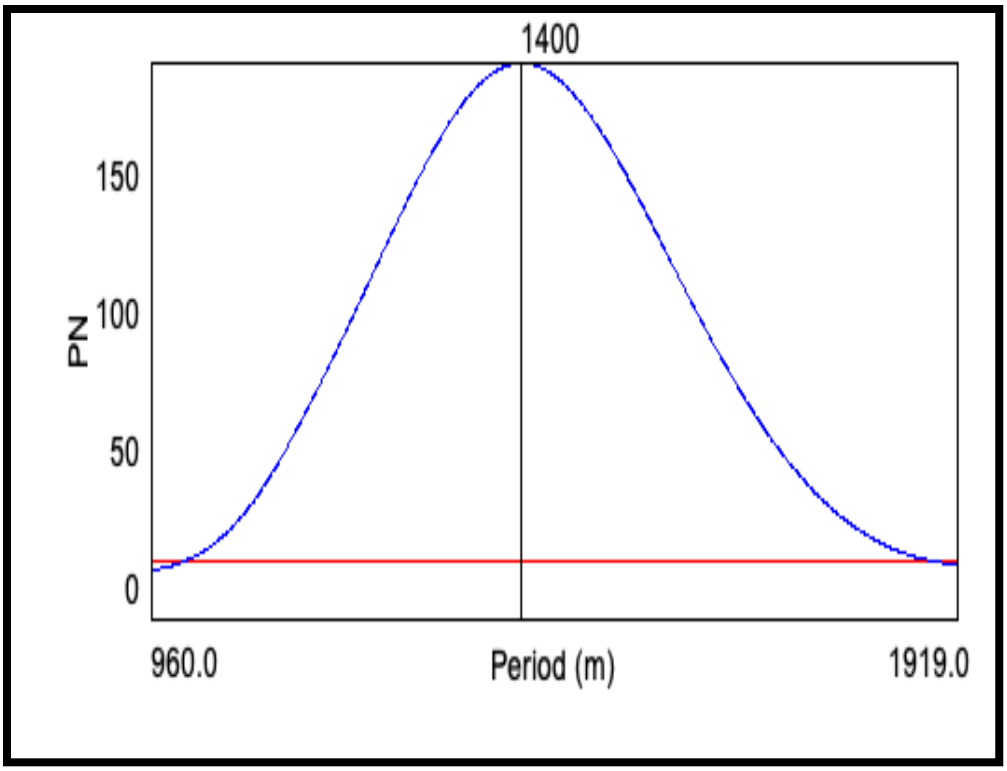

Figure 25. Lomb-Scargle periodogram of non-pathological control *Drosophila* maintained at 25 °C and aged 2-3 days, n=1.

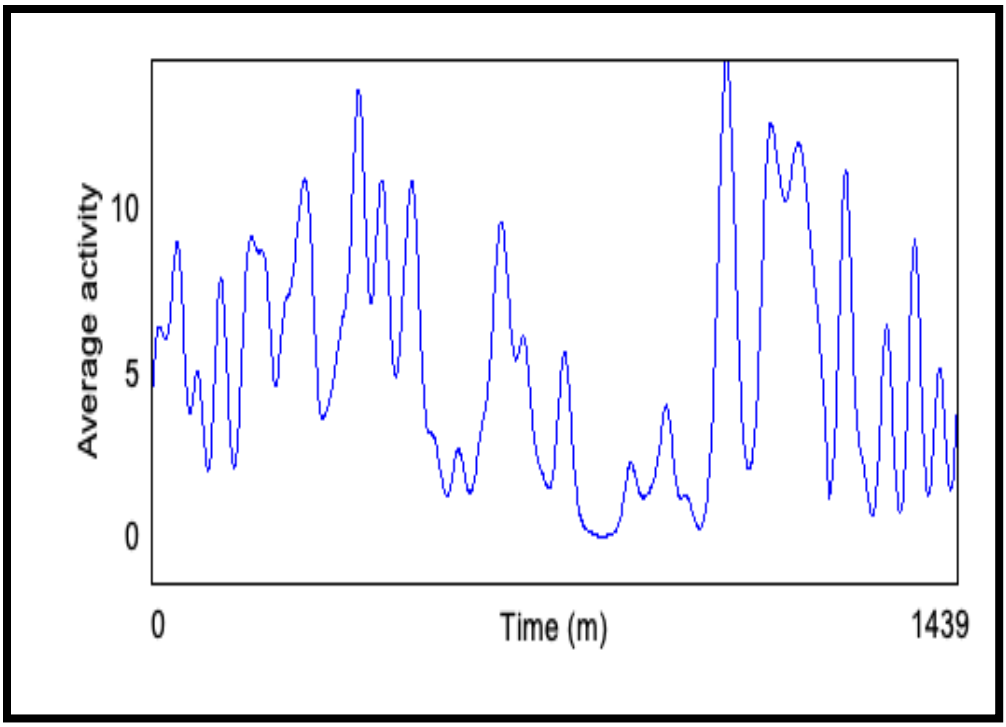

Figure 26. Average activity of pathological mutant *Drosophila* maintained at 25 °C and aged 2-3 days, n = 1.

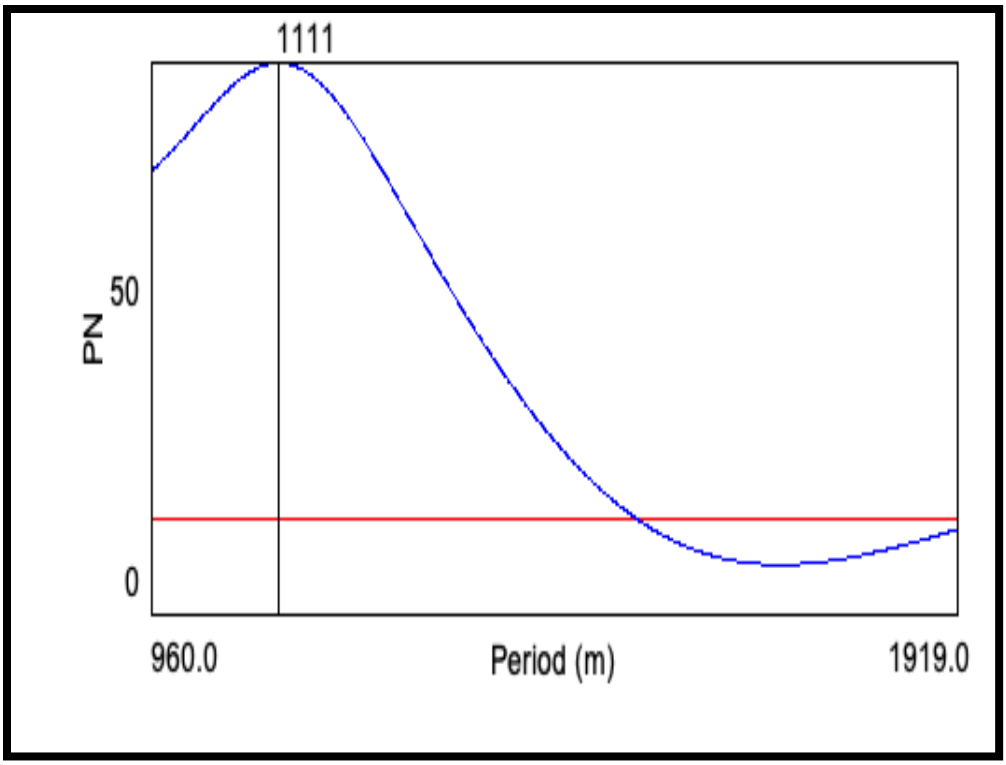

Figure 27. Lomb-Scargle periodogram of pathological mutant *Drosophila* maintained at 25 °C and aged 2-3 days, n = 1.

Chapter IV

Discussion

Studying human patients from inception of FTD pathology and subsequently through the progression of the disease is difficult. Therefore, it is imperative that research is undertaken to elucidate mechanistic insight into FTD pathology. In humans, metabolism remains stable from 20 to 60 years of age (Pontzer et al., 2021). Metabolism is influenced by circadian rhythm (Marcheva et al., 2013). Circadian rhythm changes reliably over the course of a human's life, with a trend towards becoming an early rise as a person ages (Hood, 2017). Thus, discernable changes in circadian rhythm and metabolism represent two starting points of inquiry that may elucidate clues in the progression of FTD. This study contains two different proofs of concept approaches with the aim of assessing circadian rhythm and metabolism using *Drosophila* to model FTD.

Significance of Results

The first proof of concept aimed to establish changes over time in circadian rhythm in aging *Drosophila* modeling FTD. To accomplish this, two types of data were generated from the DAM5H behavioral monitor assay. The first is an activity assay which determined the number of counts, or the number of times a *Drosophila* crossed an infrared beam while moving in the glass capillary tube (Trikinetics USA, 2023). The second is a sleep study depicted via a Lomb Scargle periodogram which according to Zechmeister and Kürster (2009), is used to investigate the repetition of data that is not

equally spaced commensurate to least-squares fitting of sine waves (Zechmeister & Kürster, 2009). The behavioral data presented on the premise that one pathological *Drosophila* is representative of five pathological *Drosophila* and one non-pathological *Drosophila* is representative of five non-pathological *Drosophila*. The five *Drosophila* from each cohort were comprised of male and female *Drosophila*. The *Drosophila* in this behavioral study exhibited a severe phenotype, meaning the symptoms of FTD were heightened and occurred at a faster rate.

Based on the Lomb Scargle graphs, this study showed a difference in circadian rhythm occurred in pathological male and female *Drosophila* (Figure 21) aged one day and maintained at 25°C compared to non-pathological male and female *Drosophila* (Figure 23) aged one day and maintained at 25°C. This study also confirmed a difference in circadian rhythm occurred in pathological male and female *Drosophila* (Figure 25) aged 2-3 days and maintained at 25°C compared to non-pathological male and female *Drosophila* (Figure 27) aged 2-3 days and maintained at 25°C. This finding is significant because it demonstrates *Drosophila* experience an altered progression in circadian rhythm, which reflects the altered progression in circadian rhythm that humans experience (Carter et al., 2019).

This study showed a difference in activity occurred in pathological male and female *Drosophila* (Figure 22) aged one day and maintained at 25°C compared to non-pathological male and female *Drosophila* (Figure 20) aged one day and maintained at 25°C. Specifically, as expected, the pathological *Drosophila* exhibited a decrease in activity compared to non-pathological *Drosophila.* This study also confirmed a difference in activity occurred in pathological male and female *Drosophila* (Figure 26) aged 2-3

days and maintained at 25°C compared to non-pathological male and female *Drosophila* (Figure 24) aged 2-3 days and maintained at 25°C. As expected, the pathological *Drosophila* had reduced activity compared to non-pathological *Drosophila*. This finding is significant as it demonstrates *Drosophila* experience a decrease in activity, which mirrors the decrease in activity FTD patients experience (McCarter et al., 2016). Therefore, we believe it is reasonable to accept these collective sleep study and activity results as a proof of concept allows researchers to progress with other investigative means of probing FTD pathology.

The second proof of concept aim, to establish a change in metabolism of *Drosophila* modeling FTD, produced unexpected results. The *Drosophila* from both the pathological and non-pathological groups were comprised of male and female *Drosophila*. As expected, there was no change in ECAR (Figure 12) between *Drosophila* pathological mutant condition (Group 1) and non-pathological control (Group 2) aged five days in and maintained at 25°C. There was also no change in OCR (Figure 13) between the *Drosophila* pathological mutant condition (Group 1) and non-pathological control (Group 2) aged five days in and maintained at 25°C. Unexpectedly, there was no change in ECAR (Figure 14) pathological mutant condition (Group 1) and non-pathological control (Group 2) aged 14 days and maintained at 25°C. A change in OCR was expected in *Drosophila* aged day 14 and maintained at 25°C. However, there was no change in OCR (Figure 15) pathological mutant condition (Group 1) and non-pathological control (Group 2) aged 14 days and maintained at 25°C.

As expected, there was no change in ECAR (Figure 16) between *Drosophila* pathological mutant (Group 1) and non-pathological control (Group 2) aged five days and

maintained at 29°C. Also as expected, there was no change in OCR (Figure 17) between *Drosophila* pathological mutant and non-pathological control aged five days and maintained at 29°C. Unexpectedly, there was no change in ECAR (Figure 18) between *Drosophila* pathological mutant (Group 1) and non-pathological control (Group 2) aged 14 days and maintained at 29°C. There was also no change in OCR (Figure 19) between *Drosophila* pathological mutant (Group 1) and non-pathological control (Group 2) aged 14 days and maintained at 29°C. The lack of change in ECAR (Figure 14 and Figure 18) and OCR (Figure 15 and Figure 19) for *Drosophila* aged 14 days and maintained at 25°C and 29°C, respectively, was unexpected as previous research has linked an age-related progressive disruption in circadian rhythm to changes in metabolism (Marcheva, 2013). Given that we confirmed a change in circadian rhythm in aged Drosophila, we expected a change in ECAR and OCR in pathological mutant *Drosophila* aged 14 days and maintained at 25°C and 29°C.

Limitations

One limitation is the medium used as a food source for *Drosophila*. The medium, consisting of ingredients such as agarose, molasses, and corn meal, is not representative of a diet that humans consume on a regular basis. This media may have effects on physiologic processes that would not otherwise occur in humans. A second limitation is human error during dissection of *Drosophila* brains. Previous firsthand experience has provided insight into the consistency of degrading brains with respect to increase length of aging. For example, compared to the brains of *Drosophila* that are a few days old, the brains of *Drosophila* aged 15-20 days become wispy and quite fragile. This creates a challenging dissection to remove the brain in one piece from the exoskeleton that the

brain is encased in. With respect to the use of the DAM5H behavioral monitor, a third limitation is the need to keep the monitor horizontal during the assay. Some adults became stuck in the media when the behavioral monitor was placed in a way that the capillary tubes were perpendicular to a level surface. A fourth limitation is the number of brains used in each group for the XFe96. If a brain becomes dislodged during the measurement, it will need to be removed from the reading. This decreases the number of samples per assay, leading to a reduction in power. As a result, making an accurate and meaningful interpretation of the results becomes difficult. In future studies, more brains should be used in anticipation of this unavoidable limitation. A fifth limitation is that this research investigated the basal level of metabolism via the XFe96 assay without any alteration of metabolic pathways.

Conclusion

The current study was undertaken to demonstrate two proofs of concept in *Drosophila* modeling FTD to justify further investigation of circadian and metabolic pathways in FTD. The current study established that the proof of concept for circadian rhythm was successful. The current study did not successfully establish metabolic proof of concept in aged *Drosophila*. Though the results were as expected for *Drosophila* aged five days, the results were not as expected for *Drosophila* aged 14 days. Therefore, the proof of concept for aged *Drosophila* should be repeated with more samples of non-pathological control and pathological mutant to rule out potential limitations prior to moving forward with other research methods. Additionally, the proof of concept for aged *Drosophila* should also be repeated with metabolic pathway drug inhibitors. The use of inhibitors would challenge brain cell functionality in *Drosophila* by altering one or more

metabolic pathways. This may yield the metabolic difference that was initially expected but not observed in the basal XFe96 metabolic analysis of pathological aged *Drosophila*.

References

Abe, Y., Yoshitane, H., Kim, D., Kawakami, S., Koebis, M., Nakao, K., Aiba, A., Kim, J., & Fukada, Y. (2022). Rhythmic transcription of bmal1 stabilizes the circadian timekeeping system in mammals. *Nature Communications*. 12, 4652.

Agilent Technologies (2023a) as referenced at http://download.chem.agilent.com/videos/Transient_Microchamber.mp4

Agilent Technologies (2023b) as referenced at https://www.agilent.com/cs/library/training/public/5991-8695EN_XF_Phenotype_Test_factsheet.pdf

American Chemical Society (2023) as referenced at https://www.acs.org/education/resources/highschool/chemmatters/past-issues/archive-2014-2015/the-science-of-sleep.html

Anderson, K., Hatfield, C., Kipps, C., Hastings, M., Hodges, J. (2009). Disrupted sleep and circadian patterns in frontotemporal dementia. *European Journal of Neurology*. 16, 317-323.

Atilano, M., Gronke, S., Niccoli, T., et al. (2021). Enhanced insulin signaling ameliorates *C9ORF72* hexanucleotide repeat expansion in *drosophila. eLife*. 10, e58565.

Balendra, R., & Isaacs, A. (2018). *C9ORF72* mediated ALS and FTD: multiple pathways to disease. *Nature Reviews Neurology*. 14, 544-558.

Baradaran-Heravi, Y., Broeckhoven, C., van der Zee, J. (2020). Stress granule mediated protein aggregation and underlying gene defects in the FTD-ALS spectrum. *Neurobiology of Disease*. 134, 104639.

Boucher, J., Kleinridders, A., & Kahn, C. (2014). Insulin receptor signaling in normal and insulin-resistant states. *Cold Spring Harbor Perspectives in Biology*. 6, a009191

Braems, E., Swinnen, B., Bosch, L. (2020). *C9ORF72* loss-of-function: a trivial, stand-alone or additive mechanism in C9 ALS/FTD? *Acta Neuropathologica*. 140, 625-643.

Brand, A., & Perrimon, N. (1993). Targeted gene expression as a means of altering cell fates and generating dominant phenotypes. *Development*. 118, 401-415.

Carter, B., Justin, H., Gulick, D., & Gamsby, J. (2021). The molecular clock and neurodegenerative disease: a stressful time. *Frontiers in Molecular Biosciences*. 8, 644747.

Dedeene, L., Schoor, E., Vandenberghe, R. Van Damme, R., Poesen, K., & Thal, D. (2019). Circadian sleep/wake-associated cells show dipeptide repeat protein aggregates in *C9ORF72*-related ALS and FTLD cases. *Acta Neuropathologica Communications.* 7, 189.

Diehl-Schmid, J., Grimmer, T., Drzezga, A., Bornschein, S., Riemenschneider, M., Forstl, H., Schwaiger, M., & Kurz, A. (2007). Decline of cerebral glucose metabolism in frontotemporal dementia: a longitudinal 18F-FDG-PET study. *Neurobiology of Aging*. 28, 42-50.

Duffy, J. (2022). *GAL4* system in *Drosophila*: a fly geneticist's Swiss army knife. *Genesis*, 34, 1-15.

Freibaum, B., & Taylor, J. (2017). The role of dipeptide repeats in *C9ORF72* related ALS-FTD. *Frontiers in Molecular Neuroscience*. 10, 35.

Garrett, L., & Niccoli, T. (2022). Frontotemporal dementia and glucose metabolism. *Frontiers in Neuroscience*. 16, 812222.

Goodman, L., & Bonini, N. (2019). Repeat-associated non-AUG (RAN) translation mechanisms running into focus for GGGGCC-repeat associated ALS/FTD. *Progress in Neurobiology*. 183, 101697.

Hantzidiamantis, P., Awosika, A., & Lappin, S. (2022). Physiology, glucose. as referenced at https://www.ncbi.nlm.nih.gov/books/NBK545201/

Hautbergue, G., Castelli, L., Ferraiuolo, L., et al. (2017). SRSF1-dependent nuclear export inhibition of *C9ORF72* repeat transcripts prevents neurodegeneration and associated motor deficits. *Nature Communications* (8), 16063.

Hood, S., & Amir, S. (2017). The aging clock: circadian rhythms and later life. *The Journal of Clinical Investigation*. 127, 437-446.

Jakšić, A., & Schlötterer, C. (2016). The interplay of temperature and genotype on patterns of alternative splicing in *drosophila melanogaster*. *Genetics*. 204, 315-325.

Lai, Y., Reina-Gonzalez, P., Maor, G., Miller, G., & Sarkar, S. (2023). Biotin rescues manganese-induced parkinson's disease phenotypes and neurotoxicity. *bioRxiv*. Preprint.

Mattis, J., & Sehgal, A. (2017). Circadian rhythms, sleep, and disorders of aging. *Trends Endocrinology & Metabolism*. 27, 192-203.

Marcheva, B., Ramsey., K.M., Peek, C. B., Affinati, A., Maury, E., & Bass, J. (2013). Circadian clocks and metabolism. *Handbook of Experimental Pharmacology*. 217, 127-155.

McCarter, S., St Louis, E., Boeve, B. (2016). Sleep disturbances in frontotemporal dementia. *Current Neurology and Neuroscience Reports*. 16, 85.

Miko, I. (2008). Thomas hunt morgan and sex linkage. *Nature Education*. 1, 143.

Molón, M., Dampc, J., Maximenko, M., Zebrowski, J., Moloń, A., Dobler, R., Durak, R., Skoczowski, A. (2020). Effects of temperature on lifespan of *drosophila melanogaster* from different genetic backgrounds: links between metabolic rate and longevity. *Insects.* 11, 470.

National Institute on Aging (2023) as referenced at https://www.nia.nih.gov/health/frontotemporal-disorders/what-are-frontotemporal-disorders-causes-symptoms-and-treatment#:~:text=There%20are%20three%20types%20of,PPA)%2C%20and%20movement%20disorders.

Neville, K., Bosse, T., Klekos, M., Mills, J., Weicksel, S., Waters, J., & Tipping, M. (2018). A novel ex vivo method for measuring whole brain metabolism in model systems. *Journal of Neuroscience Methods*. 296, 32-43.

Piper, M., & Patridge, L. (2018). *Drosophila* as a model for ageing. *Biochimica et Biophysica Acta Molecular Basis of Disease*. 1864, 2707-2717.

Pontzer, H., Yamada, Y., Sagayama, H., et al. (2021). Daily expenditure through the human life course. *Science.* 373, 6556.

Sarkar, S., Murphy, M., Dammer, E., Olsen, A., Rangaraju, S., Fraenkel, E., & Feany, M. (2020). Comparative proteomic analysis highlights metabolic dysfunction in α synucleinopathy. *Nature.* 40, 3424.

Sha, S., Takada, L., Rankin, K., et al. (2012). Frontotemporal dementia due to *C9ORF72* mutations. *Neurology*. 79, 1002-1011.

Smeyers, J., Banchi, E., & Latouche, M. (2021). *C9ORF72*: What it is, what it does, and why it matters. *Frontiers in Cellular Neuroscience.* 15, 1-16.

Tolwinski, N. (2017). Introduction: *drosophila*- a model system for developmental biology. *Journal of Developmental Biology*. 5, 9.

Trikinetics USA (2023) as referenced at https://www.trikinetics.com/Downloads/DAM5H%20Data%20Sheet.pdf

Tran, H., Almeida, S., Moore, J., Gendron, T., Chalasani, U., Lu, Y., Du, X., Nickerson, J., Petrucelli, L., Weng, Z., Gao, F. (2015). Differential toxicity of nuclear rna

foci versus dipeptide repeat proteins in a *drosophila* model of *C9ORF72* FTD/ALS. *Neuron.* 87, 1207-1214.

Wang, E., Thombre, R., Shah, Y., Latanich, R., & Wang, J. (2021). G-quadruplexes as pathogenic drivers in neurodegenerative disorders. *Nucleic Acids Research*. 49, 4816-4830.

Wang, J., Haeusler, A., & Simko, E. (2015). Emerging role of RNA DNA hybrids in *C9ORF72*-linked neurodegeneration. *Cell Cycle*. 14, 526-532.

Zechmeister, M., & Kürster, M. (2009). The generalised Lomb Scargle periodogram. *Astronomy & Astrophysics*. 496, 577-584.